Delft University of Technology, faculty Mechanical Engineering June 27 2025

Designing a **comfortable** and **secure** arm fixation for **robotic upper limb assessment** in stroke rehabilitation

Proof of concept: Using a vacuum brace for robotic assessment with the Shoulder Elbow Perturbator

Jet Meijers

TU Delft

Thesis – MSc Biomedical Engineering,, Track Musculoskeletal Biomechanics

Designing a comfortable and secure arm fixation for robotic upper limb assessment in stroke rehabilitation

Proof of concept: using a vacuum brace for robotic assessment
with the Shoulder Elbow Perturbator

Author: Jet Hester Meijers
Student number: 4855787

In partial fulfilment of the requirements for the degree of

Master of Science

in *Biomedical Engineering*

Track: Neuromusculoskeletal Biomechanics

at Delft University of Technology

to be defended publicly on Tuesday, July 8, 2025 at 13:00

Supervisors: Dr. ir. Arno Stienen, Karien ter Welle (daily, PhDc)
Thesis committee: Dr. ir. Arno Stienen (chair), Prof. dr. Frans van der Helm,
Jonathan van Zanten (PhDc)

Table of contents

Designing a comfortable and secure arm fixation for robotic upper limb assessment in stroke rehabilitation

Abstract— Background and research objective - **Approximately 80% of stroke patients experience upper limb motor impairments, including spasticity, muscle weakness, and abnormal synergies, which complicate daily activities. Accurate quantification of motor impairments is essential for optimizing rehabilitation strategies after a stroke. Objective and automatic assessment can be achieved with robotic devices. The Shoulder Elbow Perturbator (SEP) applies controlled mechanical perturbations to assess elbow and shoulder impairments. During these measurements, the wrist is fixated using plastic clamps with foam padding. But these clamps cause discomfort, positioning inconsistencies, instability, and unintended hand movemen. This study aims to design and evaluate an alternative fixation method for securing the arm in the SEP.**

Method and results - **A design thinking approach was applied. During brainstorming, concepts focused on arm conformity, rigidity, load distribution, and unrestricted elbow rotation. Based on a Harris profile, a lightweight vacuum brace was developed into a functional prototype, and clamps were redesigned to fit the brace. Validation experiments were performed with eight healthy participants tested in the SEP with both the vacuum brace and original rigid clamps. Comfort was assessed via questionnaire. Additionally, SEP angle and torque, and arm motion capture data were collected. The vacuum brace significantly reduced discomfort from severe to slight. SEP and motion capture data showed comparable fixation stability during multisine tasks. During passive stretch trials, lower intraclass correlation coefficients for stiffness estimation increased elbow displacement, and occasional movement within the clamps were observed with the brace, indicating reduced fixation performance.**

Conclusions - **The vacuum brace improved participant comfort during robotic assessment of upper limb motor impairments. Fixation stability was comparable during multisine perturbation tasks but reduced during stretch tasks, likely due to the current clamp design.**

I. INTRODUCTION

A. Motor impairments in post-stroke patients

Stroke, also known as a Cerebrovascular Accident (CVA), is a leading cause of adult disability in Europe [1] and a major cause of mortality worldwide [2]. Stroke survivors often deal with various motor impairments, including muscle weakness, spasticity, and abnormal muscle synergies [3]. Spasticity is a motor disorder characterized by a velocity-dependent increase in muscle tone and exaggerated stretch reflexes [4]. Muscle synergies are coordinated activation patterns of muscles during movement. Healthy synergies are often disrupted as a consequence of the stroke lesion, while atypical or inefficient synergies develop due to cortical reorganization and the emergence and upregulation of alternative descending pathways [5]. Approximately 80% of stroke patients experience some degree of motor impairment in the upper limbs [6]. This leads to discomfort and significant difficulties in daily activities such as personal care, eating, drinking, and managing household responsibilities [7]. For example, arm spasticity hampers smooth, controlled motion required for tasks such as dressing or eating. Similarly, abnormal synergies, such as involuntary coupling of shoulder abduction with elbow flexion, limit the ability to perform isolated joint movements. This makes it difficult to reach, grasp, or manipulate objects independently.

Accurate quantification of motor impairments is essential for optimizing rehabilitation strategies after a CVA [6]. Currently, these impairments are assessed using various manual clinical tools, including the Modified Ashworth Scale (MAS), Modified Tardieu Scale (MTS), and the Fugl-Meyer Assessment (FMA) [8]. Despite their widespread use, these assessments are subjective and dependent on the observations and scoring of the examiner. This introduces limitations such as poor reliability, restricted validity, and a lack of detailed information [8]–[11]. These issues highlight the strong need for more objective, valid, and reliable methods to assess motor impairments [10, 12, 13].

B. Robotic assessment: Shoulder Elbow Perturbator

Robotic devices equipped with advanced sensors and control systems present a novel and effective approach for quantifying motor impairments in post-stroke rehabilitation. These devices facilitate semi-automated assessments, offering a promising alternative to traditional manual clinical evaluations. Automated devices take away the subjectivity of the physician and thereby ensure more reliable results. Existing robotic devices assessing motor impairments are capable of providing objective, quantitative measurements, delivering consistent data on the motor function of a patient [12].

The Shoulder Elbow Perturbator (SEP - Hankamp Rehab, Enschede, The Netherlands, Figure 1) exemplifies such a robotic device. The SEP is designed to control the elbow joint angle while partially compensating for the weight of the arm. It incorporates a direct-drive servo motor connected to a lever that supports the forearm and facilitates controlled elbow rotation. A spring-based mechanism within the system provides compensation for shoulder abduction, thereby reducing the gravitational load on the arm. This enables the isolation and quantification of abnormal synergies between shoulder and elbow movement. The system continuously measures resistance forces and angular positions, which are then converted into elbow torque and elbow angle. These measurements allow the SEP to objectively assess muscle weakness, abnormal movement synergies, spasticity, and changes in the viscoelastic properties of the elbow joint. [14]. To enable these assessments, the SEP is capable of applying various types of mechanical perturbations during measurement tasks:

Fig. 1: A participant seated in the SEP with the forearm securely fixated with a clamp (1) and the shoulder abducted to 80°. The participant is strapped into the chair, and an emergency button is placed on the upper leg for safety [14].

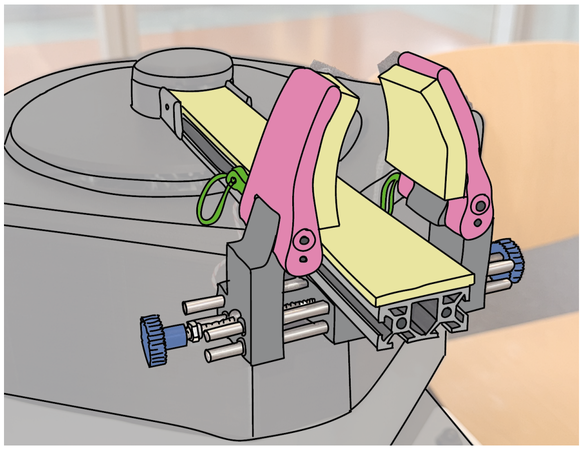

Fig. 2: Current SEP attachment configuration for securing the arm. Components: *pink*: 3D-printed clamps, *yellow*: soft foam padding, *blue*: rotating knob for clamp adjustment, *green*: emergency release mechanism.

- Free movement: The arm is allowed to move without external perturbation, allowing for baseline assessment of voluntary range of motion.
- Passive stretch: The SEP imposes slow or fast rotations of the elbow joint, typically from flexion to extension, while continuously recording the resulting resistance torque. This data allows for the estimation of parameters associated with passive tissue properties and spasticity, including joint stiffness and the detection of velocity-dependent reflex activity.
- Multisine perturbations: Low-amplitude, continuous multisine (MS) perturbations are applied to the elbow joint to excite the elbow across a broad frequency range. The resulting torque and angle data sets are used in system identification to estimate dynamic joint parameters such as inertia, damping, and stiffness, providing a detailed characterization of the mechanical response of the joint during movement.

These perturbations can be applied during various task conditions:

- Relax task: The participant is instructed to remain passive, allowing the evaluation of the mechanical properties of the joint in the absence of voluntary muscle activity.
- Resist task: The participant actively resists perturbations, increasing joint stiffness and enabling the assessment of voluntary control mechanisms.
- Targeted resistance force task: The participant maintains a predefined level of resistance force, for example by matching a visual target. This condition allows for assessment of joint behavior under controlled muscle activation.

Through these combinations of perturbation type and task condition, the SEP facilitates the detailed characterization of joint impedance mechanisms. Specifically, it enables the estimation of mechanical parameters such as joint stiffness, damping, and inertia, which are relevant to clinical phenomena including muscle weakness, abnormal synergies, spasticity, and altered viscoelasticity [15].

C. Attaching a subject in a robotic device

Effective fixation of a subject within robotic assessment devices, or rehabilitation exoskeletons, is crucial to prevent misalignment issues that negatively influence natural human limb coordination and introduce significant interaction uncertainties [16, 17].

Specifically, to perform measurements with the SEP, the forearm of the subject must be accurately aligned and securely fixated to the SEP arm. Figure 2 illustrates the attachment method of the SEP. The medial epicondyle of the elbow is positioned at the pivot point of the SEP lever, with the shoulder abducted to 80°. The wrist is secured using a 3D-printed plastic clamp lined with foam padding [14]. The clamp can be adjusted along the length of the lever to accommodate different arm lengths and includes an emergency release mechanism for safety. However, this fixation method presents several limitations:

1) Discomfort: To ensure that the arm moves in unison with the SEP lever, the clamp must be tightly secured. Anatomical variations frequently lead to localized pressure points, particularly around bony landmarks at the wrist. This causes discomfort during prolonged measurement sessions required for SEP protocols [18]. In stroke patients, compromised skin integrity and spasticity contribute to impaired blood circulation and increased skin sensitivity. These factors collectively elevate the risk of pressure-induced injuries and discomfort even more [19].
2) Positioning inconsistencies: Variability in the positioning of the clamp on the forearm and imprecise alignment between the elbow joint and the axis of rotation of the SEP can lead to a mismatch between the angular position of the arm (θ_{arm}) and that of the SEP (θ_{SEP}), as shown in Figure 3. This misalignment distorts the applied torque perturbations and can introduce measurement errors. When the subject is consistently misplaced in the SEP, these errors become systematic. When the subject is positioned differently across trials or subjects, this introduces random variability, reducing the

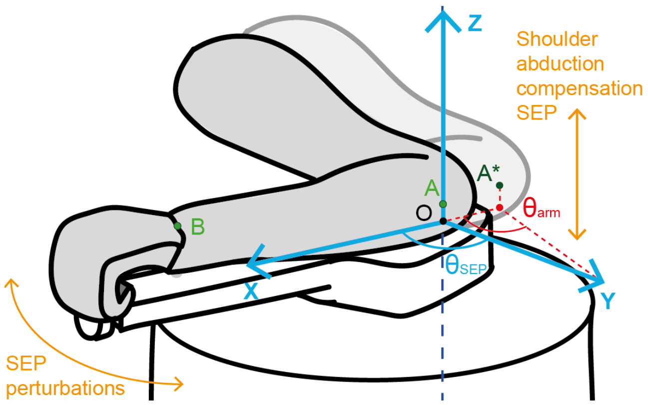

Fig. 3: Illustration of the arm of a subject positioned in the SEP, with the main movement directions of the SEP indicated in orange. Point A shows correct elbow alignment in the SEP. Point B indicates where the wrist is secured within the clamp. The effect of misalignment in the x-direction between the elbow joint (A*) and the origin of the rotational axis of the SEP (O) is shown. This misalignment causes a difference between the angular position of the arm (θ_{arm}) and that of the SEP (θ_{SEP}).

reliability and reproducibility of the measurements. Both effects limit the accuracy and consistency of measurements.

3) Instability during measurements: During applied perturbations, small shifts of the arm or elbow can occur due to insufficient fixation stability. Internal movement of the forearm within the clamp may introduce unintended dynamics, which can interfere with the accurate estimation of joint parameters
4) Hand movements: The clamps only secure the wrist, which allows for wrist abduction and adduction and permits small, unintended movements of the hand. Trembling or passive motion of the hand may introduce additional inertia or dynamic artifacts into the system, interfering with accurate joint parameter estimation.

Other robotic devices for assessing motor impairments of the upper extremity typically use straps to secure the subject within the device [20]–[22]. For the SEP, such fixation methods do not provide sufficient mechanical stability for accurate dynamics identification. Straps are partially elastic and allow minor positional shifts, preventing rigid coupling of the arm to the device. This lack of rigidity potentially introduces additional dynamic behavior that interferes with the accuracy of parameter estimations. A combination of straps and holding a joystick is commonly used in devices such as the ArmeoSpring, ArmMotus, and W-EOD [23]–[25]. But this approach is unsuitable for the SEP, as relaxation taks measurements require the arm to remain completely relaxed. Holding a joystick induces muscle activation, compromising measurement validity.

An alternative fixation method was presented by van der Krogt et al. [26], who immobilized the wrist using a custom-fitted fiberglass cast. This provides both comfort and secure attachment. Yet, producing and applying fiberglass casts is time-consuming and requires specialized removal tools such as a cast saw. Furthermore, they are not reusable, making them impractical and costly for repeated use in clinical settings, where efficiency, cost-effectiveness, and sustainability are essential.

D. Research goal

This thesis project aims to design and validate an attachment method that securely fixes and accurately aligns the arm of the patient in the Shoulder Elbow Perturbator, while maintaining comfort during robotic assessment. The design must be practical and suitable for clinical environments, including rehabilitation centers and hospitals. Improving the attachment system will enhance the reliability and clinical applicability of the SEP by enabling accurate, repeatable, and patient-friendly assessments of motor impairments in the upper limb.

The attachment should be optimized for key measurement scenarios commonly performed with the SEP, such as slow and fast passive stretch movements and continuous multisine perturbations, under varying task conditions including relaxed, resistive, and targeted resistance force tasks. Performance will be evaluated and compared to the original fixation method based on patient comfort and the technical quality of the measurements, focusing on positional stability and reproducibility.

II. DESIGN

A. Method

A design thinking approach was employed to develop a suitable attachment design for the SEP. This methodology consists of six distinct phases: empathize, define, ideate, prototype, test, and implement [27]. In the context of this project, the process progressed up to and including the test phase. The approach was iterative, enabling transitions back to earlier stages when necessary. This flexibility supported a deeper understanding of user needs, refinement of the problem definition, and ongoing improvement of proposed solutions throughout the design process.

B. Requirements

After analyzing the problems of the current fixation method and the functionalities of the SEP, a comprehensive list of requirements and preferences was compiled. The requirements represent essential user needs that must be met for any proposed concept to be considered viable. Some requirements are associated with corresponding preferences, which describe desirable features that can further enhance the design and distinguish a good solution from an excellent one. Each requirement is categorized to indicate its origin or purpose within the project. The requirements were refined throughout the design process based on new insights and practical considerations. Table I presents the final list of requirements and preferences.

TABLE I: Overview of design requirements and preferences

	Subject	Requirement	Preference	Category
1.	Fixation	The design must ensure that the pivot point of the elbow of the patient (Figure 3, point A) remains within a tolerance of ±1 cm of the pivot point of the SEP (Figure 3, point O) in the Z-plane throughout the measurements.	The design should minimize the displacement of the pivot point of the elbow of the patient (point A) in the Z-plane throughout measurements. Aiming for 0 cm displacement relative to the pivot point of the SEP (point O, Figure 3).	Measurement accuracy
		The design must ensure that the wrist of the patient (point B, Figure 3) remains within a positional tolerance of ±1 cm relative to the SEP lever in the y-direction, and within a rotational tolerance of ±5° for supination/pronation and wrist ab/adduction during measurements.	The design should minimize wrist displacement (Figure 3, point B) during measurements, targeting 0° pronation/supination and 0 cm y-direction displacement relative to the SEP lever. It must also minimize unintended dynamic hand motion caused by oscillations.	Measurement accuracy
2.	Patient configuration	The design must ensure that the arm of the patient is supported in a relaxed, passive position, with the elbow flexed and the forearm either pronated or demi-pronated. With the elbow (Figure 3, point A) and wrist (Figure 3, point B) within ±1 cm tolerance of the SEP lever in the Z-plane.	Patients should be configured in the SEP as consistently as possible, ensuring repeatable alignment and reliable measurements.	Measurement accuracy
3.	Comfort	The design must ensure that the patient can remain positioned in the SEP for at least 30 minutes without experiencing physical pain lasting more than 30 minutes after the session.	The design should optimize comfort for individuals after stroke by minimizing pressure points, preventing skin irritation or shear, and maintaining proper circulation during prolonged fixation.	Comfort
4.	Attachment time	The attachment process should not last more than 5 minutes.	The attachment time should be as short as possible.	Feasibility
5.	Weight	The design must not exceed 2 kg.	The design should be as lightweight as possible to avoid influencing SEP measurements.	Measurement accuracy
6.	Inertia	-		Measurement accuracy
7.	Sustainability	-	The design should be as sustainable as possible, using durable materials and allowing for repeated use across patients.	Sustainability
8.	Hygiene	The design must comply with MDR hygiene standards [28].	The design should be as easy and quick to clean as possible.	Regulations
9.	Costs	-	The manufacturing and implementation costs should be as low as possible.	Feasibility
10.	Interference	The design must not interfere with the movements of the SEP (indicated by the orange arrows in Figure 3) or with the associated joint movements of the participant, including shoulder abduction, internal and external rotation, and elbow flexion and extension.	-	Measurement accuracy
11.	Mechanical failure	The design must withstand 40 Nm torque generated by the SEP without failure.	-	Feasibility
12.	Patients	The design must fit wrists circumferences from 13–21 cm [29] and forearms lengths from 21.87–31.6 cm (P5–P95 population, [30]). Patients with open wounds or skin conditions are excluded.	-	Feasibility
13.	Safety	The patient must be released from the SEP within 10 seconds in case of emergency, in line with MDR requirements.	-	Regulations

C. Brainstorming

To generate ideas for the design, a structured brainstorming session was conducted, complemented by an exploration of existing fixation methods in similar robotic measurement devices. The ideation process focused on ensuring precise alignment of the elbow and arm, and achieving a secure yet comfortable fixation of the forearm within the SEP. During the brainstorming phase, the problem was divided into two distinct components: a force-distributing element for the arm of the subject (force distribution component) and a mechanism that attaches the arm securely to the SEP (attachment component). This division was deemed necessary, as designing the attachment mechanism without first understanding the interface with the arm would be impractical. Initial efforts concentrated on creating the force distribution component. This component would later be integrated into the separate attachment component. Sketches and ideas forming the design landscape are shown in Appendix A.

The three most promising ideas for the force distribution component were evaluated using a Harris profile [31], considering the seven predefined preferences in Table I. Additionally, a personalized

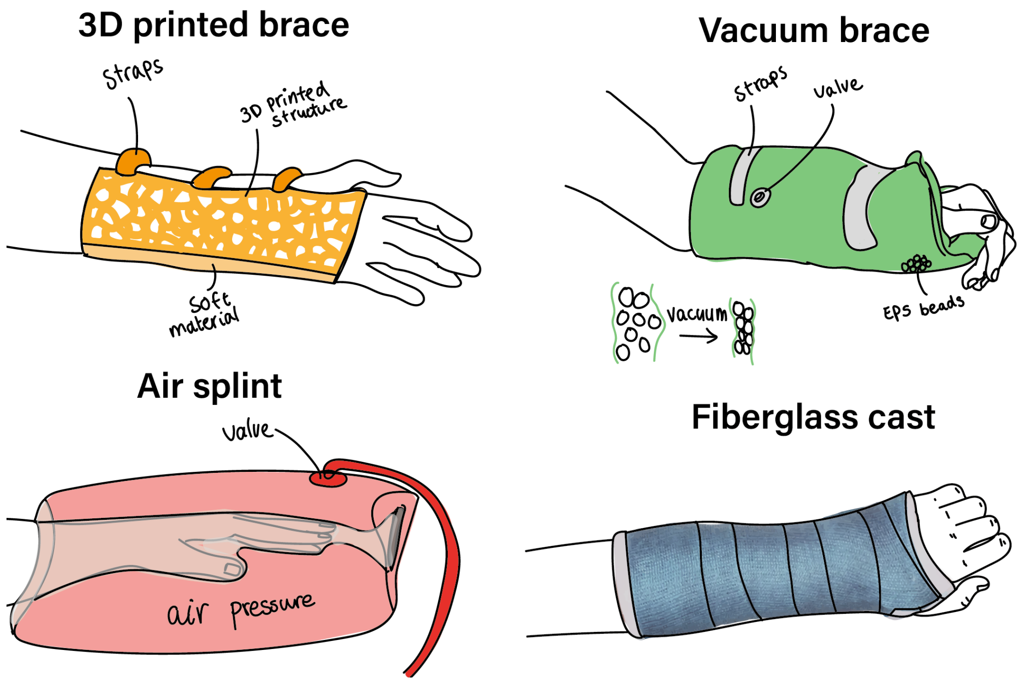

Fig. 4: Illustrations of the concepts used for the Harris profile

fiberglass cast, used in similar robotic research applications, was evaluated using the same Harris profile. This ensured that the proposed designs aimed to improve upon a personalized fiberglass cast. The evaluated concepts, shown in Figure 4, are:

- General 3D Printed Brace: This concept involves a standardized wrist brace 3D-printed using a rigid plastic material. The brace would be available in three standard sizes to accommodate different arm dimensions. The brace is reusable and can be cleaned with a wipe between uses. However, it is not custom-fitted to individual users, which may result in pressure points or poor fit for some patients, potentially reducing the degree of fixation.
- Vacuum Brace: The vacuum brace is an existing concept [32]–[35] that consists of a vacuum bag filled with expanded polystyrene (EPS) beads. This flexible bag is wrapped around the arm of the patient and secured. Air is evacuated from the bag using a specialized pump, causing it to stiffen and mold to the arm of the patient. This principle would be adapted to ensure compatibility with the SEP system.
- Inflatable air Splint: An air splint is another existing concept [36]. It consists of a double-walled, airtight cylindrical material placed around the forearm of the patient. A pump inflates the splint through a connected tube, causing it to expand and conform to the wrist of the patient. When sufficiently pressurized, the wrist is immobilized, but this might compromise blood circulation. This concept would also be modified to make it suitable for use with the SEP.
- Fiberglass Cast: Fiberglass casts are commonly used for immobilizing joints or limbs, such as in the case of fractures [37]. The process involves wetting a fiberglass roll, which is then applied over a sleeve around the wrist of the patient. The fiberglass molds to the arm, dries, and hardens. This concept is non-reusable and must be custom-applied and removed with a special cast saw for each individual.

Based on educated guesses, the Harris profiles were completed, as shown in Appendix B. The analysis indicated that the vacuum brace concept demonstrated the highest overall potential. Consequently, this design was selected for further development in the prototyping phase.

D. Prototyping

Existing vacuum braces (CME - Vacuüm armspalk, Meber - Halley 884, PAX - Vacuümspalk voor onderarm, Schmidt GmbH - RESCUEFORM OPTIVAC 2.0, Ambulancemed - Vacuum splint set, Ferno Norden - Vacuum splint set Blue line) are generally large, with the shortest models measuring approximately 45 cm. These braces often extend beyond the hand and over the elbow. This would restrict elbow movements, limiting the range of motion during SEP measurements and compromising measurement quality. To meet the predefined requirements, a prototype vacuum brace was developed to assess the feasibility of this concept.

A series of iterative prototypes was developed, each refined based on identified limitations and implemented improvements. Throughout this process, the design was continuously evaluated against the defined requirements, and different design choices were made to optimize performance. A summary of the different prototype iterations is shown in Appendix C. Design choices and validation steps in the prototype process will be explained in the following sections: Dimensions, Fixation, Patient configuration, and Attachment component.

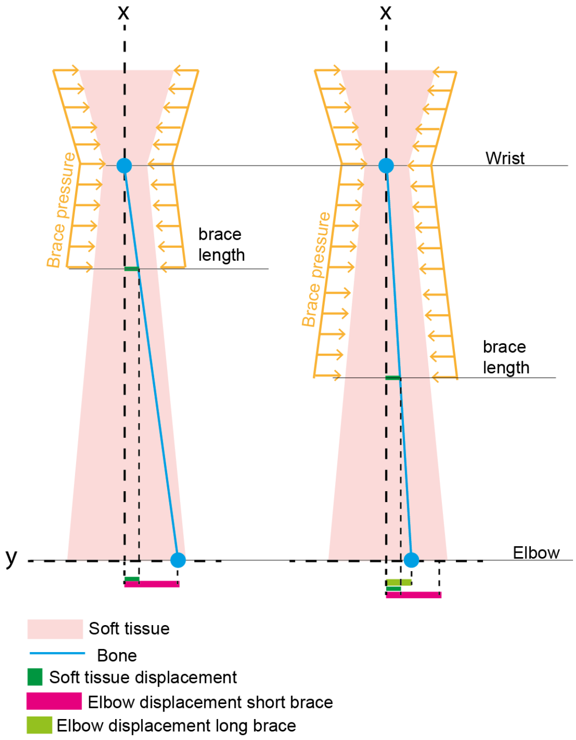

Fig. 5: Illustration of elbow displacement under short and long brace configurations, assuming identical soft-tissue shift at the proximal end of each brace.

E. Dimensions

The determination of the brace length was based on a combination of anthropometric data, mechanical force distribution, soft tissue behavior, and extrapolation. A brace can apply a finite pressure to the wrist before discomfort occurs. Increasing the brace length distributes this pressure over a larger area, improving comfort and enhancing restriction of unwanted forearm motion. As illustrated in Figure 5, assuming identical soft-tissue shift, a longer brace better restricts elbow displacement due to extrapolation. For these reasons, a brace that extends proximally as far as possible is preferable from a stability and force distribution perspective

Yet, the brace must not obstruct elbow flexion during SEP measurements. To ensure adequate forearm support without limiting elbow flexion, the final dimensions were based on anthropometric data from the 5th percentile female and 95th percentile male populations [38].

Derived from the 5th percentile female forearm length of 21.87 cm [30], the proximal length of the brace was limited to approximately two-thirds of this value, resulting in 14 cm from the wrist. This provides sufficient support without interfering with elbow flexion. To minimize undesired hand dynamics during measurements, a distal extension was added to support the hand. Based on 95th percentile male hand dimensions, the wrist-to-grip length was estimated at 8.6 cm [30]. The distal extension was set to 10 cm to provide partial support. Combined with the 14 cm proximal length, this resulted in a total brace length of 24 cm.

To account for variations in forearm dimensions, the brace circumference was based on elbow circumference data. According to McDekker et al. [39] the range is approximately 25.2 to 33.0 cm. To accommodate this range and material thickness, the circumference was set to 35 cm. For individuals with smaller arms, overlapping material ensures a secure and adjustable fit.

F. Fixation

As outlined in the design requirements, undesirable movements include wrist pronation/ supination, adduction/abduction, and forearm translations relative to the SEP lever. To prevent these degrees of freedom, the fixation must eliminate such motion within the brace itself. This can be achieved by ensuring that the brace conforms closely to the geometry of the arm of the subject and subsequently becomes rigid upon vacuum extraction of air from the EPS bead-filled vacuum chamber.

The quantity of EPS beads inside a vacuum bag determines the stiffness of the brace after vacuum application. However, to meet comfort requirements and ensure practical mounting to the SEP, the brace should not be excessively thick. Increased thickness leads to heat retention and complicates attachment procedures. Based on these considerations and preliminary manual testing, a thickness of 2 cm was selected, corresponding to approximately 1300 ml of EPS beads.

Initial bending tests on a flat, vacuum-sealed bag showed that the EPS beads tended to distribute unevenly, creating stiff regions with high density and weak zones with low material concentration. To mitigate this, a compartmentalised inner structure made of elastic fabric was introduced to ensure an even distribution of EPS beads. Vertical compartments improved bead distribution, but significantly reduced transverse stiffness, making the brace prone to folding along its circumference.

Rotating the compartments by 45 degrees into a diagonal layout resulted in balanced stiffness in both directions, with a longitudinal modulus of 1.29 MPa and a transverse modulus of 1.20 MPa. This configuration provided sufficient structural stability. The full bending test calculations and results are presented in Appendix E.

To properly shape the brace to the contour of the arm before applying vacuum, circumferential drawstrings were used. Although the flat material is relatively stiff, it lacks shape stiffness when wrapped around the arm, allowing it to shift or fold over itself. To prevent this, structural straps were added to reinforce the U-shape into a rigid, closed O-shape, providing the necessary cylindrical form stiffness. Three structural straps and clamps were positioned proximally, distally, and at the wrist to maintain overall stiffness and prevent deformation.

G. Patient configuration

To achieve consistent wrist alignment within the brace, several methods were evaluated. Based on considerations of simplicity, versatility, and ease of cleaning, a single reference line was selected. This line, drawn in contrasting color on both the inner and outer surfaces at the level of the wrist indents, ensures correct wrist positioning within the brace. The external reference line also enables alignment of the brace with the SEP attachment, ensuring consistent positioning of the arm relative to the device. Details on the evaluated alignment methods are provided in Appendix F.

H. Attachment component

During prototype development, it became evident that the existing SEP clamp mechanism could be retained, requiring only dimensional adaptation to the vacuum brace geometry. Accordingly, the clamp was redesigned in SolidWorks with an increased diameter and grip length. Based on the 35 cm circumference of the vacuum brace, a clamp diameter of 10 cm was selected to accommodate the brace. To enlarge the contact area and enhance fixation stability, the clamp width was extended to 8 cm. The final clamp geometry is presented in Appendix G. These dimensional modifications were used for the fixation of the vacuum brace in the SEP.

I. Final design

The prototyping phase resulted in the final vacuum brace design and the redesigned clamps. Figure 6 provides an overview of the final design, including its main components. The drawstrings are used to conform the brace to the shape of the arm. The straps with integrated clamps ensure a strong O-shape. The alignment indication line is included to position both the wrist and the clamps accurately. The valve is located to allow easy connection to the vacuum pump while avoiding interference during use. Additionally, a small pocket is incorporated to store the excess length of the drawstrings, preventing entanglement during SEP perturbations. The redesigned clamp was 3D printed in PLA with a high infill density to maximize strength. After support removal, the red alignment line was added for positioning of the vacuum brace inside the clamps. Detailed step-by-step instructions for fitting the brace to the forearm are available in Appendix H, and a full description of the fabrication process and details are presented in Appendix I.

III. **VALIDATION**

A. Experiment

To evaluate whether the vacuum brace outperforms the existing attachment method in terms of fixation stability, hand movements, and patient comfort, a small-scale experiment was conducted. During this experiment, both the existing design and the newly developed vacuum brace prototype were tested and compared under identical conditions. For this experiment, an HREC amendment for the existing HREC of the SEP was requested and approved.

B. Participants

Eight healthy participants (ages 20–62), including three males and five females, were recruited for the experiment. All participants were right-handed, had no history of elbow impairment, and provided informed consent after reading the participant information document (Appendices J and K) before participation. The participants represented a range of arm dimensions, as listed below:

- Wrist circumference: 15–18 cm
- Forearm circumference: 21–27.5 cm
- Forearm length: 23–31 cm

C. Materials

The Shoulder Elbow Perturbator was used as the robotic device to apply mechanical perturbations and perform all measurements in this study.

An OptiTrack motion capture system (NaturalPoint Inc.) equipped with three cameras was set up to ensure complete visibility of the arm of the participant from all relevant angles. This system detects and identifies reflective markers within the capture volume, enabling high-precision tracking of arm movements during SEP measurements.

D. Experiment setup

Reflective markers were placed on anatomical landmarks to track elbow position, forearm rotation, and hand displacement. Whenever possible, markers were positioned on bony landmarks to maximize accuracy and reproducibility. At least three markers per segment were used to form clusters, identifying body segments [40]. In cases where the brace interfered with placement on the fingers, the distal finger markers were shifted slightly toward more accessible locations. Markers were positioned on the left and right sides of the clamp to track the movement of the SEP lever. Due to obstruction from the wrist clamps, markers could not be placed directly on the wrist. Figure 7 (A) illustrates the marker configuration used:

1) Acromion process of the shoulder
2) Lateral epicondyle of the elbow
3) Olecranon of the elbow
4) Forearm: as distal as possible within the constraints of the brace
5) Left and right sides of the SEP clamp
6) Base of the index finger
7) Base of the ring finger
8) First knuckle of the middle finger

The arrangement of the OpiTrack cameras ensured optimal coverage and marker visibility throughout the measurement process. The setup of the experiment and OptiTrack cameras is shown in Figure 7 (B).

E. Protocol

Before starting measurements with a participant, two reflective markers were attached to the SEP. One marker was placed at the pivot point of the lever, and the other at the distal end of the lever. A short motion

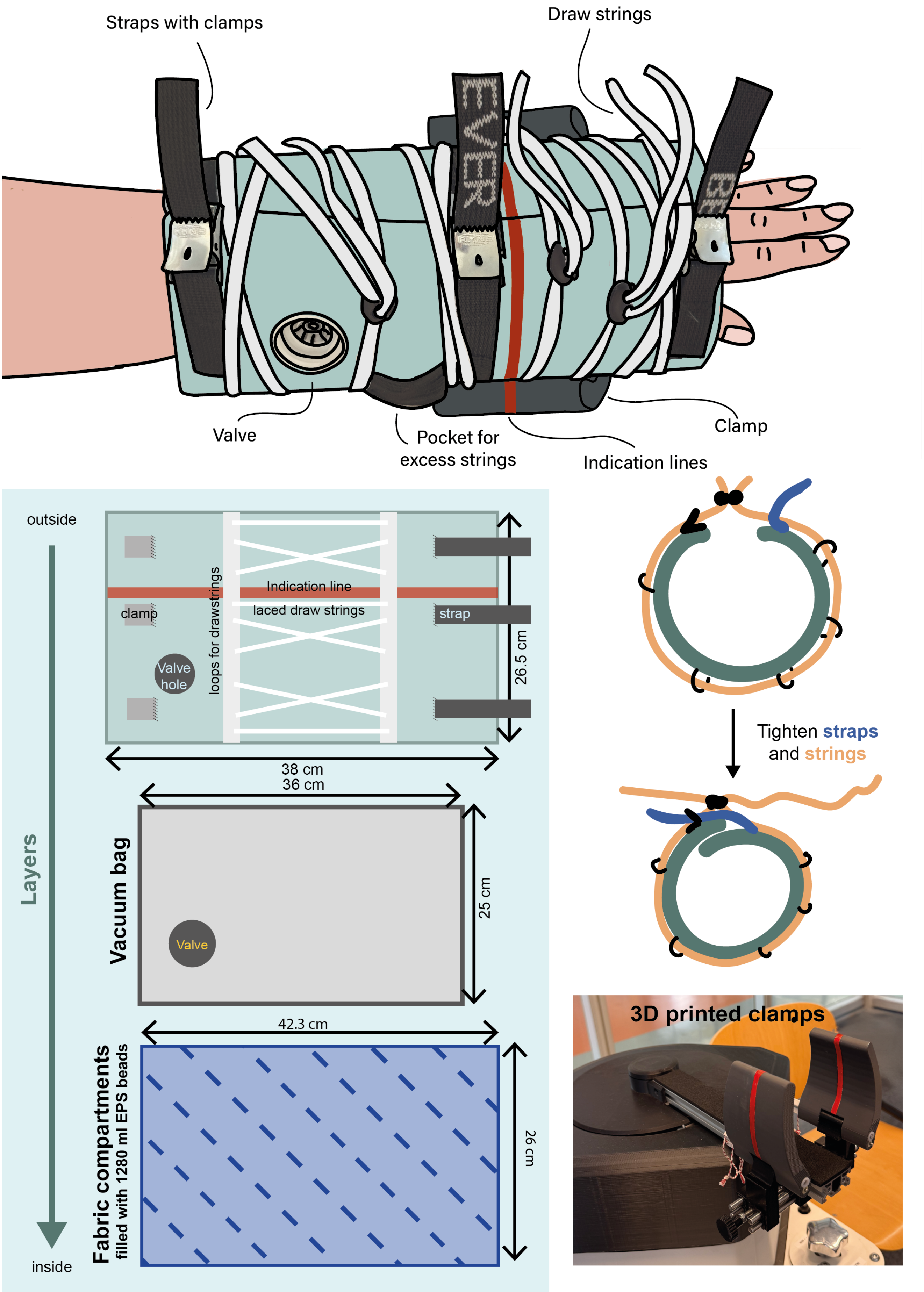

Fig. 6: Overview of the final vacuum brace and clamp design.

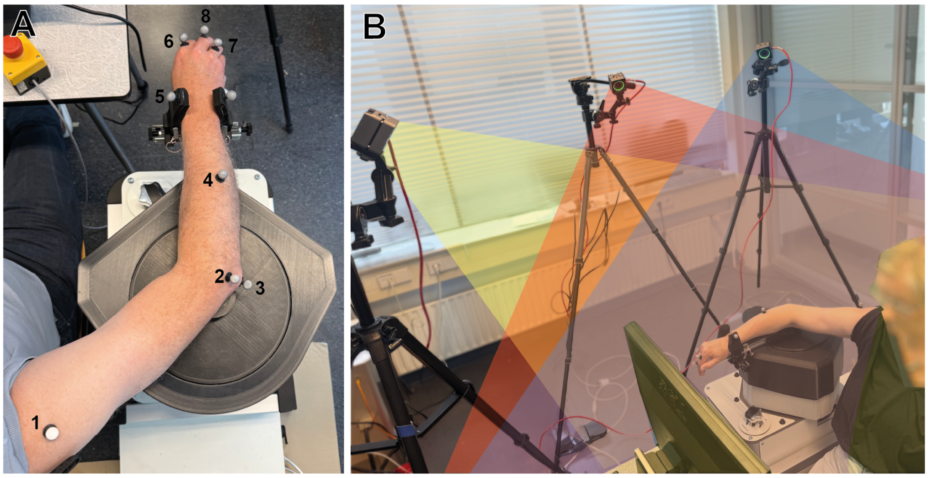

Fig. 7: A: Marker placement on the arm and hand of the participant during SEP measurements. B: Experimental setup showing the three OptiTrack cameras and their tracking volume. A participant is positioned in the SEP, looking at a monitor containing feedback during the measurements.

capture recording was taken to ensure the spatial positioning of the SEP lever was identified.

Participants were encouraged to ask questions and informed that they should immediately report any pain or significant discomfort during the testing procedure. Each participant performed the SEP measurement protocol twice: once with the original clamp-only setup and once with the vacuum brace and redesigned clamps. The order of these tests was randomized for each participant. For hygiene and practical reasons, a tubular arm bandage was first placed on the arm before the brace was applied, as described in Appendix H.

Wrist circumference, forearm circumference, and forearm length were measured using a standard measuring tape and noted for each participant. Reflective markers were attached to the participant at predefined locations. The participant was seated in a stationary chair positioned next to the SEP. The right arm of the participant was placed into the SEP at an abduction angle of approximately 80 degrees and a flexion angle of approximately 70 degrees. The medial epicondyle of the elbow was aligned with the pivot point of the SEP lever. The wrist clamp was adjusted to the length of the arm, in case the participant was wearing the vacuum brace, the red indication lines were aligned with those on the clamp. The clamps were tightened securely at the wrist, providing firm attachment without causing more than mild discomfort.

The SEP measurement protocol included the following steps:

- Setting the maximal flexion and extension angles.
- Maximum voluntary torque (MVT) measurements: Three trials of 5 seconds each, with 10 seconds of rest between trials, and a rest period of 30 seconds at the end.
- Multisine relaxation task: One trial of 220 seconds, using a 5° amplitude multisine velocity perturbation containing logarithmically spaced frequencies between 0.1 and 50 Hz with equal power at all frequencies. Followed by a rest period of 30 seconds at the end.
- Multisine resistance tasks: Two trials of 120 seconds each, using a 5° amplitude multisine torque perturbation containing logarithmically spaced frequencies between 0.1 and 50 Hz with equal power at all frequencies. 30 seconds of rest between trials and at the end.
- Stretch tests: Six trials of passive elbow stretching from flexion to extension at two speeds (6°/s and 200°/s) and three activation levels (0%, 25%, and 50% of the MVT). Each combination was repeated three times. A rest period of 15 seconds was provided between each combination.

Visual feedback was provided on a monitor. During the maximal voluntary torque testing the monitor showed when the participant should give their maximal force. During the stretch tests, the target force was displayed alongside the actual force exerted by the participant. This allowed the participant to adjust their effort in real time.

After finishing the measurement protocol, participants were then asked to complete a short questionnaire (Appendix L) consisting of Likert-scale items and open-ended questions regarding their comfort during the measurement.

F. Data analysis

Using Microsoft Excel, Matlab, and Motive, data analysis of the results from the experiments focused on the predefined attachment issues:

1) Discomfort

Comfort of the participant during measurements is assessed using the data from the comfort questionnaire:

- Likert-scale ratings: For each questionnaire item, the mean score was calculated for both the clamp-only and vacuum brace conditions. Two-sided Student t-tests were performed to assess whether differences in ratings between conditions were statistically significant.
- Open-ended responses: Answers were qualitatively reviewed to identify the origin of discomfort and specific protocol phases with peak discomfort.

Additionally, the mean maximum voluntary torque of all participants was compared between the clamp-only and vacuum brace conditions using two-sided Student t-tests. Reduced torque during the initial MVT measurements could occur due to pain or discomfort experienced by the participant.

2) Instability during measurements

To evaluate stability during measurements, differences between the measurements with and without the vacuum brace were analyzed across several aspects: translational displacement of the elbow, supination and pronation of the forearm, system identification data quality during multisine perturbation tasks, and the repeatability of stiffness estimation in the stretch tasks.

OptiTrack marker trajectories were used to quantify elbow displacement relative to the SEP pivot point. For each trial, the position of the lateral epicondyle marker in the XY plane was evaluated with respect to the SEP pivot marker. To assess elbow movement stability independently from the accuracy of initial alignment on the SEP pivot, the velocity of the epicondyle marker in the Z-plane was computed. The root-mean-square (RMS) of this velocity was calculated for each task using the formula below, where N denotes the number of samples within a given task, and v represents the instantaneous velocity in the Z-plane:

$$\mathrm{RMS}(v) = \sqrt{\frac{1}{N}\sum_{i=1}^{N} v_i^2} \tag{1}$$

To evaluate forearm supination and pronation, OptiTrack marker trajectories of the forearm and the left and right clamps of the SEP were used. A coordinate system was constructed based on these markers to determine the anatomical rotation axis of the forearm and compute torsion over time. For each task, the maximum supination and pronation angles were calculated for both conditions: clamp-only and with the vacuum brace. A detailed description of the coordinate system definition and the computational procedure is provided in Appendix M.

For the MS perturbation tasks, power cross-spectral densities (S) between signals were estimated using Welch averaging. For the relax task data (220 seconds), the first and last 10 seconds were discarded, after which 10 segments of 20 seconds with rectangular windows were used. The same approach was applied to the resist task data (120 seconds), resulting in 5 segments of 20 seconds after removing the first and last 10 seconds. Frequency-response functions (FRF, H) and coherence (γ^2) were subsequently derived as follows:

- MS relax task: Using the rotation angle of the SEP (θ), the measured torque (T) during the perturbations, and the MS rotation perturbation from the SEP data ($d\theta$), the FRF was defined as:

$$H_{\text{relax}} = -\frac{S_{\theta\, d\theta}}{S_{T\, d\theta}} \tag{2}$$

- MS resist task: This was calculated in the same manner as the MS relax task, but using the MS perturbation torque from the reference signal (dT). The FRF was defined as:

$$H_{\text{resist}} = -\frac{S_{\theta\, dT}}{S_{T\, dT}} \tag{3}$$

- Coherence:

$$\gamma^2 = \frac{|S_{\theta\, T}|^2}{S_{\theta\,\theta} \cdot S_{T\,T}} \tag{4}$$

Mean values and standard deviations (SD) were calculated across all participants. These were evaluated qualitatively to assess potential differences between measurements with and without the vacuum brace.

The six stretch tasks were each repeated three times. For each stretch, the elbow stiffness $K(t)$ was determined as:

$$K(t) = \frac{T(t)}{\theta(t)} \tag{5}$$

Stiffness was estimated by fitting a linear line to the extension phase of each stretch and extracting the slope of this line. This slope represents the stiffness for that specific trial. Stretches were excluded from analysis if identified as invalid based on observed participant error or disproportionately irregular torque data, as determined through visual inspection.

For each task condition, the intraclass correlation coefficient ICC(2,k) of these stiffness values was calculated across all participants. The ICC values for measurements with and without the vacuum brace were evaluated.

3) Hand movements

To evaluate whether the use of the vacuum brace influences hand oscillations during measurements, and thereby might affect system identification, the OptiTrack markers placed on the hand and fingers were analysed. This analysis was performed during the MS relax task, as the hand is expected to introduce the most additional dynamics when relaxed and exposed to random multisine perturbations.

The analysis involved tracking the x- and y-position of finger markers relative to the right clamp marker. To eliminate the influence of differences between the larger and smaller clamp designs, the RMS velocity of the finger markers relative to the right clamp marker was calculated across all participants. These values were compared between conditions with and without the vacuum brace.

Finally, potential differences in apparent inertia with and without the brace were explored by inspecting the FRF magnitude in the higher frequency range of the MS perturbation tasks.

IV. VALIDATION RESULTS

A. Comfort

As shown in Figure 8, the average overall comfort rating without the brace was 3.6 (severe discomfort), compared to 1.9 (slight discomfort) with the brace, indicating a significant reduction in discomfort ($p = 0.000212$). Responses to the comfort questionnaire per participant are provided in Appendix N. All participants

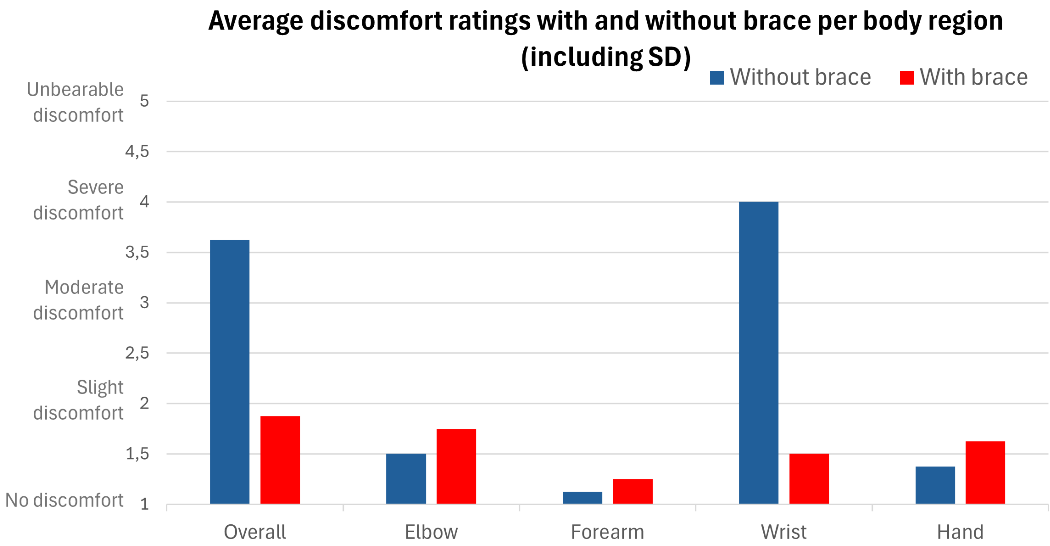

Fig. 8: Bar plots of mean discomfort scores from the comfort questionnaire.

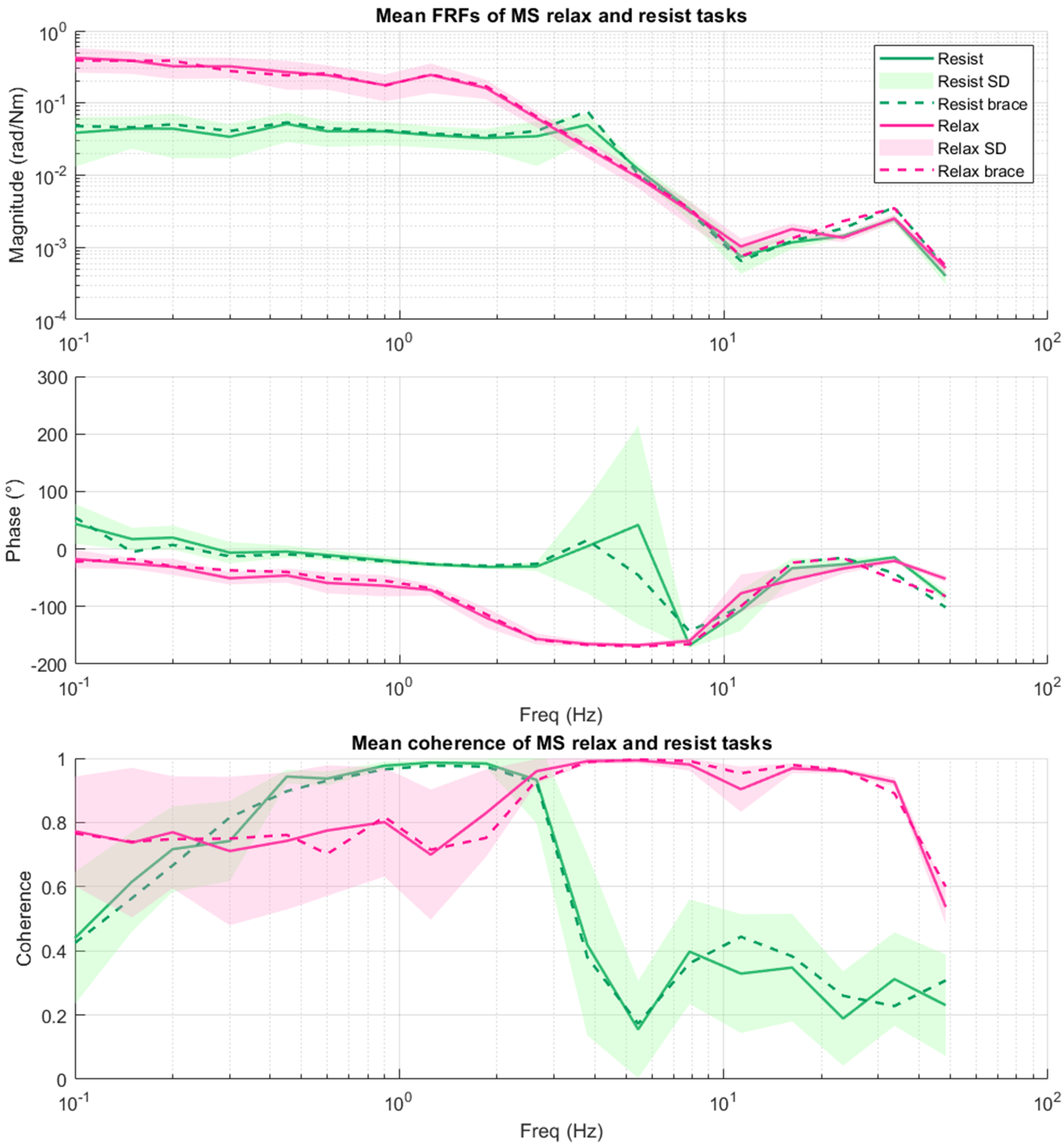

Fig. 9: Mean Frequency-response functions and coherence and standard deviation (SD) of the multisine relax and resist tasks.

TABLE II: Data analysis results per task - Mean RMS of epicondyle velocity w.r.t. SEP pivot point, Mean maximal forearm supination/pronation (°), Mean RMS of finger velocity w.r.t. right clamp during MS relax task (mm/s), and Intraclass coefficients (ICC(2,k) of stiffness estimations of stretch tasks

Task	RMS of epicondyle marker velocity (mm/s)		Max. forearm supination (°)		RMS of finger marker velocity mm/s			ICC(2,k) of estimated stiffness	
	Without brace	With brace	Without brace	With brace	Finger	Without brace	With brace	Without brace	With brace
Multisine relax	6.84	6.79	0.36	2.01	Index Middle Ring	20.78 25.40 19.71	12.04 14.18 11.62		
Multisine resist	19.54	17.66	1.45	4.08					
Slow stretch relax	10.23	12.30	4.79	5.68				0.92	0.93
Slow stretch 25% MVT	9.88	10.99	5.20	15.49				0.61	0.51
Slow stretch 50% MVT	11.65	13.88	5.64	11.78				0.84	0.66
Fast stretch relax	21.72	19.72	5.85	10.80				0.52	0.20
Fast stretch 25% MVT	28.19	34.36	5.52	10.55				0.70	0.56
Fast stretch 50% MVT	29.34	32.44	7.30	13.63				0.69	0.10

reported a preference for measurements performed with the brace.

The most prominent difference in discomfort was observed at the wrist, where the average Likert score decreased by 2.5 points when using the brace, shifting from severe to slight discomfort ($p = 0.000122$). Discomfort was primarily attributed to pressure points at the wrist. Two participants classified wrist discomfort without the brace as “unbearable”, and one participant over 60 was unable to complete the final 50% MVT stretch trials without the brace due to pain, reporting a minor skin lesion afterward.

For other body regions (elbow, forearm, hand), no significant differences between brace and clamp-only measurements were observed ($p > 0.05$). Discomfort ratings with the brace never exceeded slight discomfort levels. Notably, the highest discomfort scores with the brace were reported at the elbow.

Discomfort most frequently occurred during stretch tests requiring force exertion. One participant reported heat buildup inside the vacuum brace as a source of discomfort.

Additionally, the average maximum voluntary torque generated during the clamp-only measurements was 23.75 Nm. During the vacuum brace measurements, this value increased to an average of 26.8 Nm. However, this difference was not statistically significant according to the t-test ($p > 0.05$). An overview of the individual maximum voluntary torque values for all participants is provided in Appendix O.

B. Motion capture arm movements

Table II presents the results of data analysis, including the RMS values of the lateral epicondyle displacement relative to the SEP pivot point. The results show that, for the multisine tasks, RMS values with the brace are comparable to or slightly lower than those without the brace. In contrast, for most stretch tasks, RMS values are higher when the vacuum brace is used. To provide additional spatial context for these RMS values, Appendix O includes plots of the average elbow position in the XY plane per task, relative to the SEP pivot point.

The maximum forearm supination/pronation angles per task are included in Table II as well. These data show that measurements conducted with the brace generally resulted in slightly higher rotational angles, particularly during the stretch tasks.

The mean RMS velocity values of the fingers relative to the right clamp during the MS relax task in Table II show that across all fingers, lower RMS values were observed in measurements conducted with the vacuum brace. To provide additional spatial context for these RMS values, Appendix O includes XY-plane displacement plots of the finger trajectories relative to the right clamp during the MS relax task for an exemplary participant.

C. Technical quality of the measurements

Figure 9 shows the mean FRFs and coherence for the multisine perturbation tasks, along with the standard deviation (SD) of the clamp-only measurements. The results demonstrate that FRF magnitude, phase, and coherence are nearly identical for measurements with and without the vacuum brace, mostly remaining within the SD boundaries. This similarity is also evident at higher frequencies, where inertial effects dominate and unintended hand dynamics typically become apparent. Only at the highest frequencies does the FRF of the brace condition exceed the SD of the clamp-only measurements. Yet, these frequencies primarily reflect the intrinsic dynamics of the SEP system itself, rather than the biomechanical response of the participant, and not used in the system identification of the arm. Furthermore, a lower FRF magnitude is observed at low frequencies during the resist tasks.

Table II presents the ICC values for elbow stiffness across all stretch tasks. With the exception of the slow stretch relax task, ICC values were consistently lower in the measurements performed with the brace.

V. DISCUSSION

A. Vacuum brace prototype

The vacuum brace prototype in this study was developed as an alternative fixation method to improve both participant comfort and mechanical stability during robotic motor impairment assessment of the shoulder and elbow. The concept offers a promising approach to distribute fixation forces more evenly across the arm. Unlike conventional rigid clamps that exert high localized pressure, the vacuum brace achieves fixation by conforming a flexible structure filled with EPS beads to the shape of the arm. Once vacuum is applied, the structure stiffens, resulting in effective immobilization of the forearm and wrist using relatively low tightening forces. This improves user comfort while maintaining positional stability.

However, a concern of this prototype is the long-term durability. The EPS beads used as internal filler material may degrade over time due to clamp pressure and the repeatedly applied vacuum. Additionally, the vacuum bag material used in this prototype is vulnerable to small leaks, which can reduce internal pressure and compromise both the rigidity and fixation quality. This degradation was not investigated in the current study.

Additionally, the bending resistance of different prototypes was evaluated using simple deflection tests performed in a non-laboratory setting. While this approach supported rapid prototyping and iterative development, the absence of standardized test procedures may have affected the precision and reliability of these evaluations.

B. Motion capture considerations

Several sources of variation can affect the accuracy of marker-based motion capture and should be considered when interpreting results. Even with proper calibration, marker jitter and occlusions, particularly when gap-filling is required, can reduce reliability. Soft tissue artifacts, especially on the forearm, cause deviations between marker position and underlying bone due to skin movement, which is more pronounced in distal limb segments [41].

During vacuum brace measurements, fewer valid data points were recorded for some finger markers and clamp markers, as parts of the brace obstructed the line of sight. In addition, it was discovered after the experiments that the SEP setup was not perfectly level, with a 1.5 cm height difference between the flexion and extension extremes of the SEP lever. This is relevant during full-range stretch tasks. As elbow extension was recorded not only as displacement in the x- and y-directions but also in the z-direction. Such vertical displacement could influence forearm supination and pronation calculations, which are based on rotation matrices relative to the first valid recorded position.

Together, these factors may have introduced variability in the recorded trajectories and discrepancies in derived measures such as joint rotations or velocities. Although interpolation and filtering routines were applied to reduce their impact, these sources of error are inherent to optical tracking systems and should be considered when interpreting the motion capture results.

C. Increased comfort

The comfort questionnaire results indicate a clear preference for using the vacuum brace during SEP measurements. All participants reported the condition with the brace to be more comfortable than the measurements without. The most pronounced improvement was observed at the wrist, where the average discomfort rating decreased from 4.0 (severe discomfort) to 1.5 (slight discomfort) on the Likert scale. This reduction of 2.5 points suggests that the brace effectively mitigated the most discomfort-prone contact region during testing. The discomfort at the wrist in the clamp-only condition, classified as unbearable by two participants, highlights the limitations of using only clamps for forearm fixation.

For the other body regions, including the forearm, elbow, and hand, mean discomfort scores were slightly higher with the vacuum brace, although the differences were not significant and remained below a Likert score of 2. This may be attributed to the brace covering a larger surface area of the forearm and exerting a mild, evenly distributed pressure on the underlying tissue. Notably, the highest discomfort with the brace was reported at the elbow. This is likely explained by the altered arm position within the clamp, causing the arm to rest slightly higher than in the clamp-only condition. As a result, the forearm no longer rested fully along the SEP lever, and the primary support point shifted to the elbow. This localised contact likely created a pressure point at the elbow. Despite this effect, the average discomfort score for this region remained low at 1.75, corresponding to slight discomfort.

One participant (60+) was unable to complete the final 50% MVT stretch trials with the clamp-only measurements due to pain and subsequently reported a minor skin lesion. These findings suggest that the vacuum brace could offer clinically relevant advantages for populations more susceptible to pressure-related discomfort, such as individuals post-stroke.

Moreover, the mean maximum voluntary torque was higher with the vacuum brace (26.8 Nm) compared to the clamp-only condition (23.75 Nm), although this difference was not statistically significant ($p > 0.05$). Given the small sample size, this finding does not exclude the possibility that improved comfort with the brace may reduce pain-limited performance and thereby enhance the accuracy and reliability of muscle force assessment.

D. Fixation stability

The results in Table II provide insight into the fixation stability of the arm during SEP measurements with and without the vacuum brace. For the multisine perturbation tasks, the near-identical RMS values of the lateral epicondyle velocity indicate that the brace does not introduce additional elbow movement. Furthermore, the comparable FRFs and coherence plots presented in Figure 9 confirm that the brace does not affect system-level dynamics by introducing additional stiffness, damping, or inertia. As expected, elbow stiffness was higher during the resist tasks than during the relax condition. These findings suggest that the vacuum brace provides fixation quality during multisine perturbations that is at least equivalent to that achieved using clamp-only fixation.

During the passive stretch tasks, reduced fixation stability was observed when using the brace. Mean RMS values of the lateral epicondyle velocity were

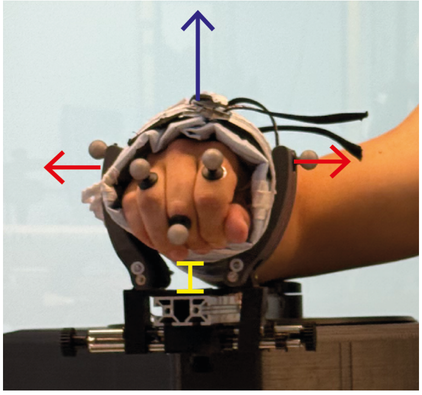

Fig. 10: Vacuum brace attached in the SEP. Outward opening of the clamps (red arrows) caused the brace to shift upward (blue arrow), resulting in the brace floating above the SEP lever surface (yellow indication).

higher in the brace condition, and ICC values for elbow stiffness estimation were generally lower, particularly during fast stretches and tasks involving a target force. These results indicate that the elbow moved more and there was reduced fixation stability during passive stretches in the vacuum brace measurements.

A likely explanation lies in the performance of the newly designed clamp used during braced measurements. The brace was observed to slightly open outward during tightening, and due to its geometry, this resulted in the brace being pushed upward (Figure 10). Once the mechanical limit was reached, further tightening no longer improved fixation, and the brace remained able to move slightly within the clamp. This movement was specifically observed during rapid elbow extension.

The increased elbow movement may also be explained by the setup procedure, in which the medial epicondyle was aligned with the SEP pivot point. As the reflective marker could not be placed directly on the medial epicondyle, it was instead positioned on the lateral epicondyle. However, the true center of rotation of the elbow lies at the anteroinferior aspect of the medial epicondyle [42], and the lateral epicondyle does not lie directly above this point. This anatomical relationship causes the position of the lateral epicondyle marker to shift relative to the pivot point during elbow flexion and extension. Which is visible in the elbow marker trajectories shown in Appendix O. The resulting displacement is particularly pronounced during stretch tasks, which involve larger flexion and extension movements, contributing to the higher observed RMS values.

Increased supination and pronation angles observed in all tasks in the brace measurements suggest that the brace allowed for more rotational movement than the clamp-only setup. This may be explained by limitations of the clamp design, which allowed the brace to move slightly in the clamps. Moreover, forearm rotation was calculated using markers on both the forearm and clamps. Small outward opening of the clamps can therefore introduce errors in the estimated angles. Although such deformation was also possible in the clamp-only condition, the smaller size and shorter length of those clamps resulted in less marker movement and thus reduced influence on the calculations. The increased angles in the brace condition likely reflect a combination of true forearm rotation and calculation artefacts.

Overall, these findings indicate that the vacuum brace maintained comparable fixation stability during multisine perturbation tasks but showed reduced stability in stretch tasks. This reduction is most likely attributable to the mechanical limitations of the redesigned, bigger clamps used in the brace measurements.

E. Reduced hand dynamics

The RMS finger velocity results in Table II suggest that the use of the vacuum brace reduces unintended movement of the hand and fingers during the multisine relax task. Lower RMS values were observed across all three fingers when the brace was applied, indicating that the added hand support provides improved distal stability beyond the fixation at the forearm.

Notably, these reductions in finger and hand movement do not affect the frequency response of the overall system. As shown in Figure 9, the FRF magnitudes at higher frequencies, relevant for estimating inertial characteristics during system identification, remain nearly identical in both the brace and clamp-only conditions. This suggests that unintended hand motion during multisine perturbations does not significantly influence the identified system dynamics. Moreover, the addition of the vacuum brace and larger clamps does not introduce noticeable changes in system inertia or damping.

F. Recommendations

1) Design improvements

From a design perspective, several improvements can be made to enhance the functionality and usability of the vacuum brace.

First, the current drawstring mechanism for shaping the brace around the arm could be replaced with an elastic tightening system. This would simplify the application process and reduce setup time. To further improve user comfort, the addition of a soft elbow cushion could help reduce localized pressure during measurements.

To facilitate consistent elbow alignment within the SEP, a small magnetic alignment aid could be implemented. This would consist of a magnetic sticker placed on the medial epicondyle of the elbow and a corresponding magnet located at the SEP pivot point, allowing for accurate positioning through tactile feedback.

Air leakage is a critical point of failure in the vacuum brace. Future designs could incorporate puncture-resistant materials for the airtight interior, along with a basic system for detecting and sealing minor leaks. Additionally, the surface material in contact with the arm should provide a comfortable sensation on the skin and be easy to clean with disinfectant wipes. The brace should ultimately be manufactured using medical-grade materials through a professional

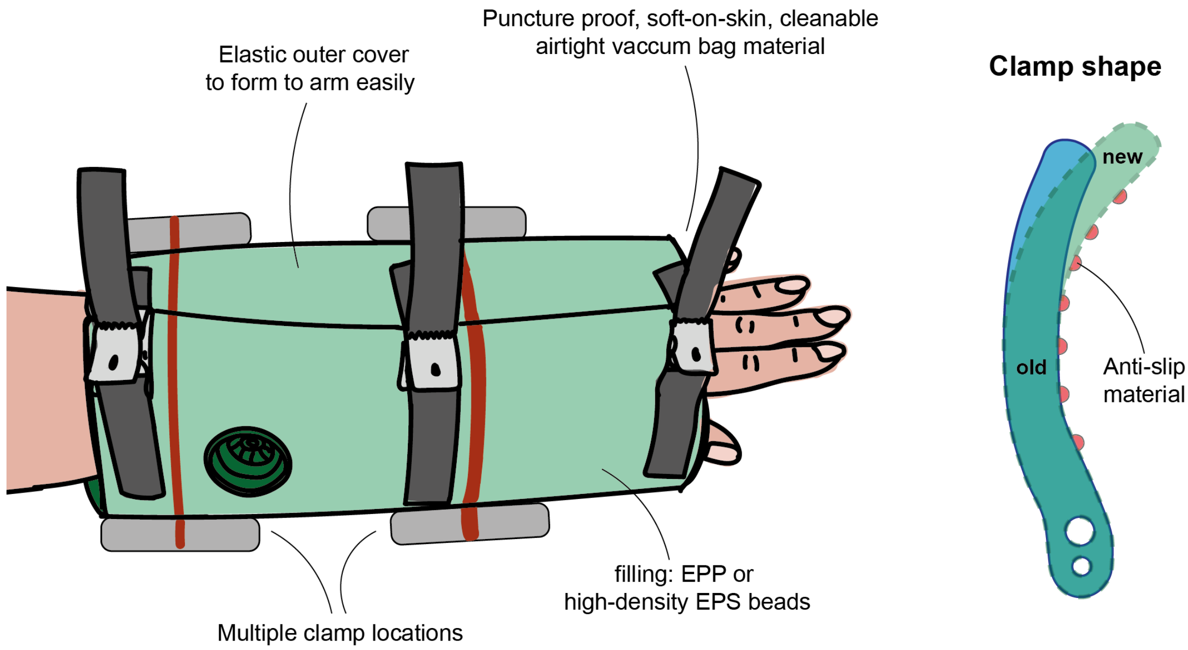

Fig. 11: Sketches of design recommendations

production process to enhance clinical applicability and long-term durability.

Further investigation is needed to assess whether a transition from standard EPS beads to harder variants such as expanded polypropylene (EPP) or high-density EPS could improve structural stiffness without increasing overall thickness, thereby enhancing fixation performance.

Lastly, the fixation clamp design should be reconsidered. The current configuration allowed the brace to be displaced upward during tightening, limiting the achievable fixation. Improved fixation could be achieved by modifying the clamp geometry, adding anti-slip surfaces, or using multiple clamp points to distribute the holding force more evenly. This would likely enhance the positional stability of the brace during SEP measurements. Figure 11 shows conceptual sketches of recommended improvements for the vacuum brace and the clamp.

2) Future research

To explore the generalizability and clinical relevance of the vacuum brace, future studies should include a larger and more diverse participant sample, including stroke patients. Evaluating the brace in a clinical population would provide essential insight into its practical utility and usability. It would also be relevant to compare the vacuum brace with fiberglass cast fixation during SEP measurements. In addition, feedback from medical professionals, such as rehabilitation physicians and therapists, is needed to assess feasibility in clinical workflows and to identify potential barriers to implementation.

To assist with consistent placement, alignment indicators were added to the brace and clamps. Nevertheless, positional inconsistencies of subjects in the SEP were not explicitly assessed in the present study. Future research should evaluate whether the use of alignment indicators on the brace and clamps improves consistency in wrist and elbow placement between sessions.

Finally, the potential applications of the vacuum brace extend beyond SEP measurements. Its use in other robotic or clinical measurement setups that require secure yet comfortable arm stabilization should be explored. Such studies could determine whether the vacuum brace provides a viable alternative to conventional fixation methods in broader biomechanical and rehabilitation contexts.

VI. Conclusion

In this study, an alternative fixation approach for securing the arm in the Shoulder Elbow Perturbator was designed. A lightweight vacuum brace was selected using a Harris profile as the preferred concept and developed into a functional prototype. The brace conforms to the arm of the subject and becomes rigid through vacuum pump application.

The vacuum brace prototype was tested in SEP measurements with eight participants and clearly showed improved comfort over conventional clamps. This enhanced comfort is particularly relevant for stroke patients, who often present with sensitive skin and are more prone to pressure-induced discomfort or skin irritation. During multisine tasks with the brace, fixation stability was comparable, with reduced hand motion. In stretch tasks with the brace, fixation performance was lower, likely due to clamp limitations rather than the brace design.

The vacuum brace shows promise not only for use in SEP assessments but also for broader implementation in robotic or clinical contexts that require secure yet comfortable arm stabilization. With further refinement, this approach could lead to more user-friendly and robust fixation solutions for rehabilitation and biomechanical research.

REFERENCES

[1] H. A. Wafa, C. D. Wolfe, E. Emmett, G. A. Roth, C. O. Johnson, and Y. Wang, "Burden of Stroke in Europe," *Stroke*, vol. 51, pp. 2418–2427, Aug. 2020. Publisher: American Heart Association.

[2] Feigin and L. Valery et al., "Global, regional, and national burden of stroke and its risk factors, 1990–2021: a systematic analysis for the Global Burden of Disease Study 2021," *The Lancet Neurology*, vol. Volume 23, pp. 973 – 1003, Oct. 2024.

[3] P. Raghavan, "Upper Limb Motor Impairment After Stroke," *Physical Medicine and Rehabilitation Clinics*, vol. 26, pp. 599–610, Nov. 2015. Publisher: Elsevier.

[4] A. D. Pandyan, M. Gregoric, M. P. Barnes, D. Wood, F. V. Wijck, J. Burridge, H. Hermens, and G. R. Johnson, "Spasticity: Clinical perceptions, neurological realities and meaningful measurement," *Disability and Rehabilitation*, Jan. 2005. Publisher: Taylor & Francis.

[5] A. J. C. McMorland, K. D. Runnalls, and W. D. Byblow, "A Neuroanatomical Framework for Upper Limb Synergies after Stroke," *Frontiers in Human Neuroscience*, vol. 9, p. 82, Feb. 2015.

[6] L. A. Ingram, A. A. Butler, M. A. Brodie, S. R. Lord, and S. C. Gandevia, "Quantifying upper limb motor impairment in chronic stroke: a physiological profiling approach," *Journal of Applied Physiology*, vol. 131, pp. 949–965, Sept. 2021. Publisher: American Physiological Society.

[7] Hersenletsel-uitleg, "Spasticiteit / Lichamelijke gevolgen / Gevolgen | Hersenletsel-uitleg.nl."

[8] Jet Meijers, "The reliability of robotic assessments of motor impairments in post-stroke patients: a literature review (unpublished)." Jan. 2025.

[9] D. J. Gladstone, C. J. Danells, and S. E. Black, "The Fugl-Meyer Assessment of Motor Recovery after Stroke: A Critical Review of Its Measurement Properties," *Neurorehabilitation and Neural Repair*, vol. 16, pp. 232–240, Sept. 2002. Publisher: SAGE Publications Inc STM.

[10] A. D. Pandyan, G. R. Johnson, C. I. Price, R. H. Curless, M. P. Barnes, and H. Rodgers, "A review of the properties and limitations of the Ashworth and modified Ashworth Scales as measures of spasticity," *Clinical Rehabilitation*, vol. 13, pp. 373–383, Oct. 1999.

[11] N. N. Ansari, S. Naghdi, S. Hasson, M. H. Azarsa, and S. Azarnia, "The Modified Tardieu Scale for the measurement of elbow flexor spasticity in adult patients with hemiplegia," *Brain Injury*, vol. 22, pp. 1007–1012, Jan. 2008. Publisher: Taylor & Francis _eprint: https://doi.org/10.1080/02699050802530557.

[12] S. Balasubramanian, R. Colombo, I. Sterpi, V. Sanguineti, and E. Burdet, "Robotic Assessment of Upper Limb Motor Function After Stroke," *American Journal of Physical Medicine & Rehabilitation*, vol. 91, pp. S255–S269, Nov. 2012.

[13] R. M. Maura, S. Rueda Parra, R. E. Stevens, D. L. Weeks, E. T. Wolbrecht, and J. C. Perry, "Literature review of stroke assessment for upper-extremity physical function via EEG, EMG, kinematic, and kinetic measurements and their reliability," *Journal of NeuroEngineering and Rehabilitation*, vol. 20, p. 21, Feb. 2023.

[14] L. L. van der Velden, B. Onneweer, C. J. W. Haarman, J. L. Benner, M. E. Roebroeck, G. M. Ribbers, and R. W. Selles, "Development of a single device to quantify motor impairments of the elbow: proof of concept," *Journal of NeuroEngineering and Rehabilitation*, vol. 19, p. 77, July 2022.

[15] M. van de Ruit, L. L. van der Velden, B. Onneweer, J. L. Benner, C. J. W. Haarman, G. M. Ribbers, and R. W. Selles, "System identification: a feasible, reliable and valid way to quantify upper limb motor impairments," *Journal of Neuroengineering and Rehabilitation*, vol. 20, p. 67, May 2023.

[16] N. Jarrasse and G. Morel, "Connecting a Human Limb to an Exoskeleton," *IEEE Transactions on Robotics*, vol. 28, pp. 697–709, June 2012.

[17] S. Tesfazgi, R. Sangouard, S. Endo, and S. Hirche, "Uncertainty-aware automated assessment of the arm impedance with upper-limb exoskeletons," *Frontiers in Neurorobotics*, vol. 17, Aug. 2023. Publisher: Frontiers.

[18] Q. Guan, Z. Yang, H. Lu, and S. Guo, "Analysis of Comfort during Transfer by a Dual-Arm Care Robot Based on Human Body Pressure and Surface Electromyographic Signals," *Bioengineering*, vol. 10, p. 903, Aug. 2023. Number: 8 Publisher: Multidisciplinary Digital Publishing Institute.

[19] Z. Vanaki, E. Mohammadi, K. Hosseinzadeh, B. Ahadinezhad, and H. Rafiei, "Prevalence of Pressure Injury among Stroke Patients In and Out of Healthcare Settings: A Systematic Review and Meta-Analysis," *Home Healthcare Now*, vol. 41, pp. 158–164, June 2023.

[20] P. Lum, C. Burgar, D. Kenney, and H. Van Machiel Der Loos, "Quantification of force abnormalities during passive and active-assisted upper-limb reaching movements in post-stroke hemiparesis," *IEEE Transactions on Biomedical Engineering*, vol. 46, no. 6, pp. 652–662, 1999.

[21] M. Zbytniewska, C. M. Kanzler, L. Jordan, C. Salzmann, J. Liepert, O. Lambercy, and R. Gassert, "Reliable and valid robot-assisted assessments of hand proprioceptive, motor and sensorimotor impairments after stroke," *Journal of Neuroengineering and Rehabilitation*, vol. 18, p. 115, July 2021.

[22] M. Kim, D. H. Kothari, P. S. Lum, and C. Patten, "Reliability of dynamic muscle performance in the hemiparetic upper limb," *Journal of neurologic physical therapy: JNPT*, vol. 29, pp. 9–17, Mar. 2005.

[23] N. Brihmat, I. Loubinoux, E. Castel-Lacanal, P. Marque, and D. Gasq, "Kinematic parameters obtained with the ArmeoSpring for upper-limb assessment after stroke: A reliability and learning effect study for guiding parameter use," *Journal of NeuroEngineering and Rehabilitation*, vol. 17, no. 1, 2020. Publisher: BioMed Central Ltd.

[24] F. Li, Y. Wu, and X. Li, "Test-retest reliability and inter-rater reliability of the Modified Tardieu Scale and the Modified Ashworth Scale in hemiplegic patients with stroke," *European Journal of Physical and Rehabilitation Medicine*, vol. 50, pp. 9–15, Feb. 2014.

[25] C. Selves, T. Lejeune, C. Detrembleur, M.-A. Haustrate, and G. Stoquart, "Validity and reliability of the assessment of hand flexors stiffness using a new electromechanical oscillatory device in people with stroke," *International Journal of Rehabilitation Research. Internationale Zeitschrift Fur Rehabilitationsforschung. Revue Internationale De Recherches De Readaptation*, vol. 46, pp. 170–177, June 2023.

[26] H. van der Krogt, I. Kouwijzer, A. Klomp, C. G. M. Meskers, J. H. Arendzen, and J. H. de Groot, "Loss of selective wrist muscle activation in post-stroke patients," *Disability and Rehabilitation*, vol. 42, pp. 779–787, Mar. 2020.

[27] Sarah Gibbons, "Design Thinking 101," July 2016.

[28] European Parliament, "Regulation (EU) 2017/745 of the European Parliament and of the Council of 5 April 2017 on medical devices, amending Directive 2001/83/EC, Regulation (EC) No 178/2002 and Regulation (EC) No 1223/2009 and repealing Council Directives 90/385/EEC and 93/42/EEC (Text with EEA relevance)," July 2024. Legislative Body: OP_DATPRO.

[29] Reh4Mat, "Wrist support AM-OSN-U-01/CCA | Reh4Mat - Manufacturer of modern orthopaedic devices."

[30] C. C. Gordon, C. E. Clauser, B. Bradtmiller, J. T. McCONVILLE, I. Tebbetts, and R. A. Walker, "ANTHROPOMETRIC SURVEY OF U.S. ARMY PERSONNEL: SUMMARY STATISTICS INTERIM REPORT," 1988.

[31] A. v. Boeijen, J. Daalhuizen, J. Zijlstra, R. v. d. Schoor, and Technische Universiteit Delft Faculteit van het Industrieel Ontwerpen, *Delft design guide : design methods*. Amsterdam: BIS Publishers, 2013.

[32] R. S. Hamilton and P. T. Pons, "The efficacy and comfort of full-body vacuum splints for cervical-spine immobilization," *The Journal of Emergency Medicine*, vol. 14, pp. 553–559, Sept. 1996.

[33] R. M. Letts and D. A. Hobson, "The vacuum splint: an aid in emergency splinting of fractures," *Canadian Medical Association Journal*, vol. 109, pp. 599–600, Oct. 1973.

[34] J. R. Schetrumpf, "Instant splints: Vacuum compacted polystyrene balls," *British Journal of Plastic Surgery*, vol. 26, pp. 393–397, Oct. 1973.

[35] C. M. Ward, "Vacuum splintage of the hand," *The Hand*, vol. 9, pp. 71–75, Feb. 1977.

[36] I. Capperauld, "Inflatable Splint," *BMJ Military Health*, vol. 114, pp. 87–91, Apr. 1968. Publisher: British Medical Journal Publishing Group Section: Original Articles.

[37] K. L. Kowalski, J. D. Pitcher, Jr., and B. Bickley, "Evaluation of Fiberglass versus Plaster of Paris for Immobilization of Fractures of the Arm and Leg," *Military Medicine*, vol. 167, pp. 657–661, Aug. 2002.

[38] J. Molenbroek and R. de Bruin, "Enhancing the use of anthropometric data,"

[39] M.C. Dekker and J.F.M. Molenbroek, "Data of Simona population for MDHMS application - Collecting and deriving

data for human modelling sotware to use in Flight Simulator Design," tech. rep., Dec. 1999.

[40] M. Wessling, J. Harlaar, and TU Delft, "Lecture: 3D KINEMATICS & MOTION RECORDING."

[41] Z. Bons, T. Dickinson, R. Clark, K. Beardsley, and S. K. Charles, "Compensating for Soft-Tissue Artifact Using the Orientation of Distal Limb Segments During Electromagnetic Motion Capture of the Upper Limb," *Journal of Biomechanical Engineering*, vol. 144, p. 071007, July 2022.

[42] Felix H. Savoie, "Elbow Anatomy & Biomechanics - Shoulder & Elbow - Orthobullets," Mar. 2024.

APPENDICES

Appendix A: Design landscape

This appendix presents a summary of the design landscape explored during the development of the concepts.

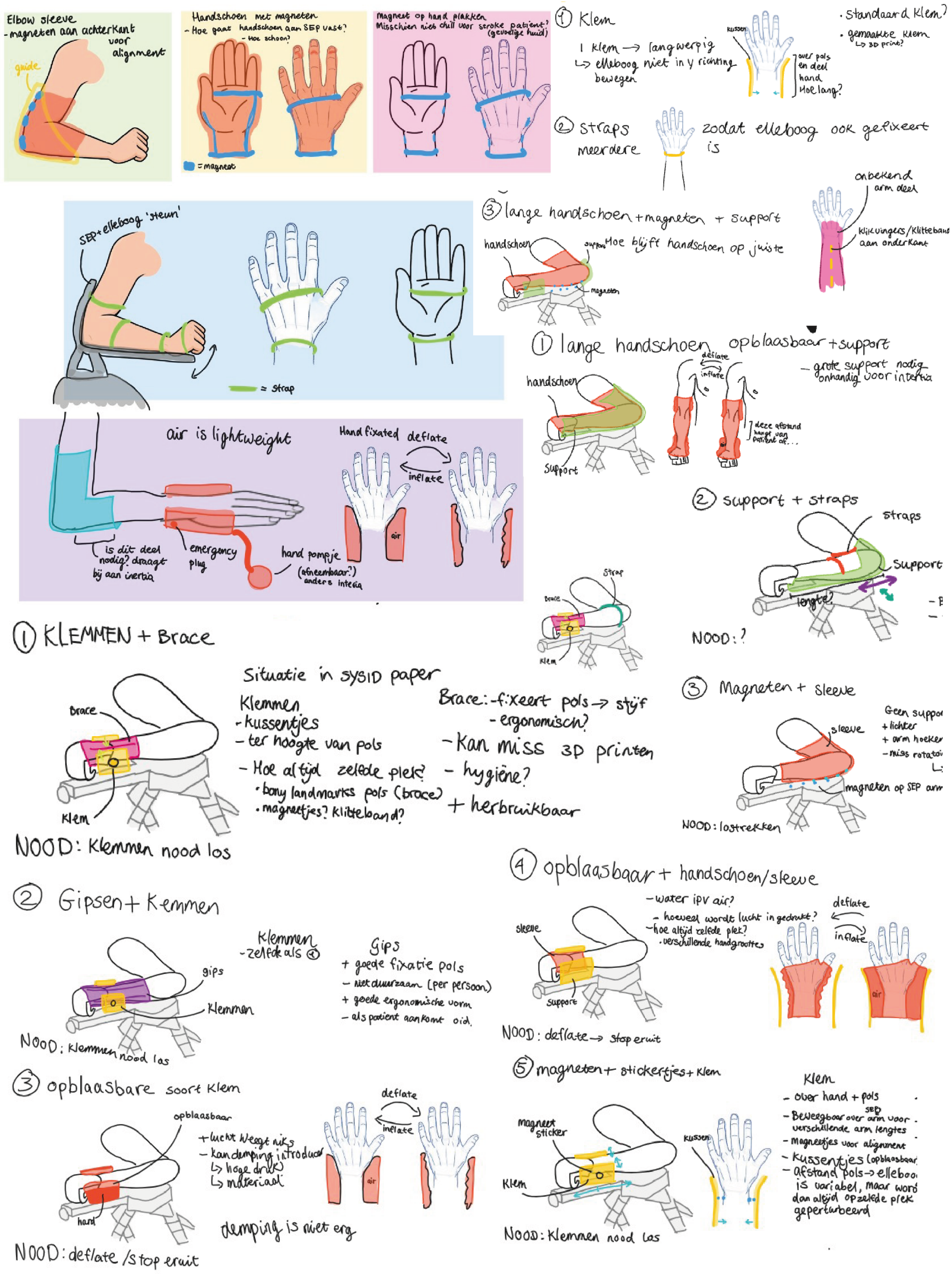

Force distribution component

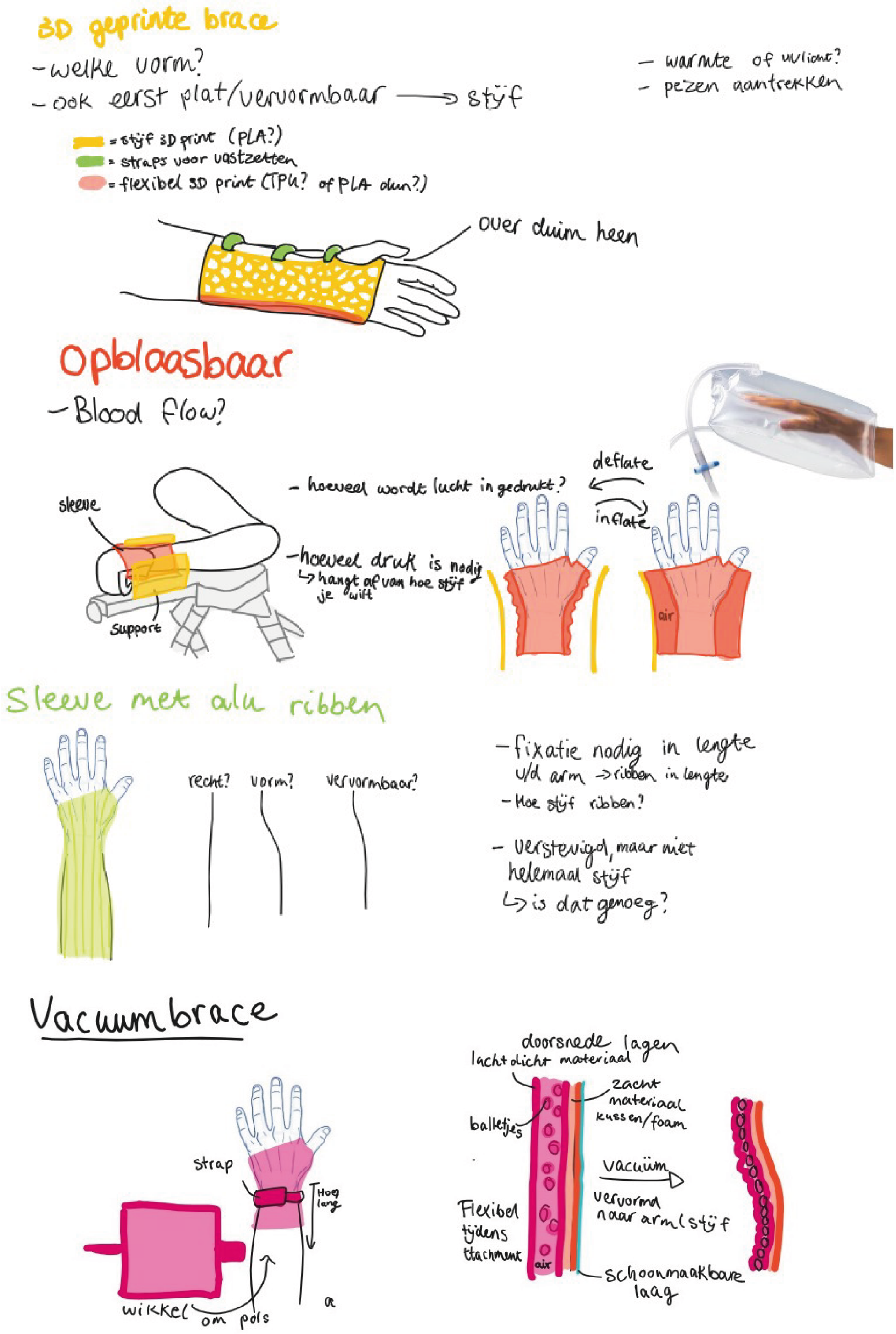

Appendix B: Harris profile evaluation

To evaluate and compare different design concepts, a Harris profile was employed. Preferences were ranked from most to least important and scored using a four-point ordinal scale: $--$ (very poor), $-$ (poor), $+$ (good), and $++$ (very good). These scores were assigned based on educated guesses and practical estimations of performance. Figure 12 displays the outcome of this assessment. Below, the scoring criteria and rationale for each preference are described.

1. Fixation

– Fixation is inadequate in two or more directions.
\- Fixation fails in one critical direction.
\+ Fixation restricts all directions, but does not conform to individual anatomy.
++ Fully immobilizes all directions using a rigid, form-fitted structure.

2. Comfort

– Causes pain during or after use.
\- Uncomfortable, but no lasting pain.
\+ Tolerable, minor pressure points possible.
++ Fully conforms to the arm and distributes pressure.

3. Attachment time

– Takes more than 5 minutes.
\- Takes 4–5 minutes.
\+ Takes 2–4 minutes.
++ Less than 2 minutes.

4. Weight and inertia

– less than 700 g.
\- 500–700 g.
\+ 200–500 g.
++ more than 200 g.

5. Sustainability

– Single-use only.
\- Reusable fewer than 10 times.
\+ Reusable, less than 10 times without degradation.
++ Durable, reusable, and low environmental impact.

6. Cleanability

– Requires specialized cleaning.
\- Can be cleaned with wipes, but time-consuming.
\+ Cleanable in under 1 minute.
++ Cleanable in under 30 seconds.

7. Cost

– Non-reusable, expensive.
\- Reusable, less than 10 times.
\+ Reusable, moderate cost.
++ Reusable and low cost.

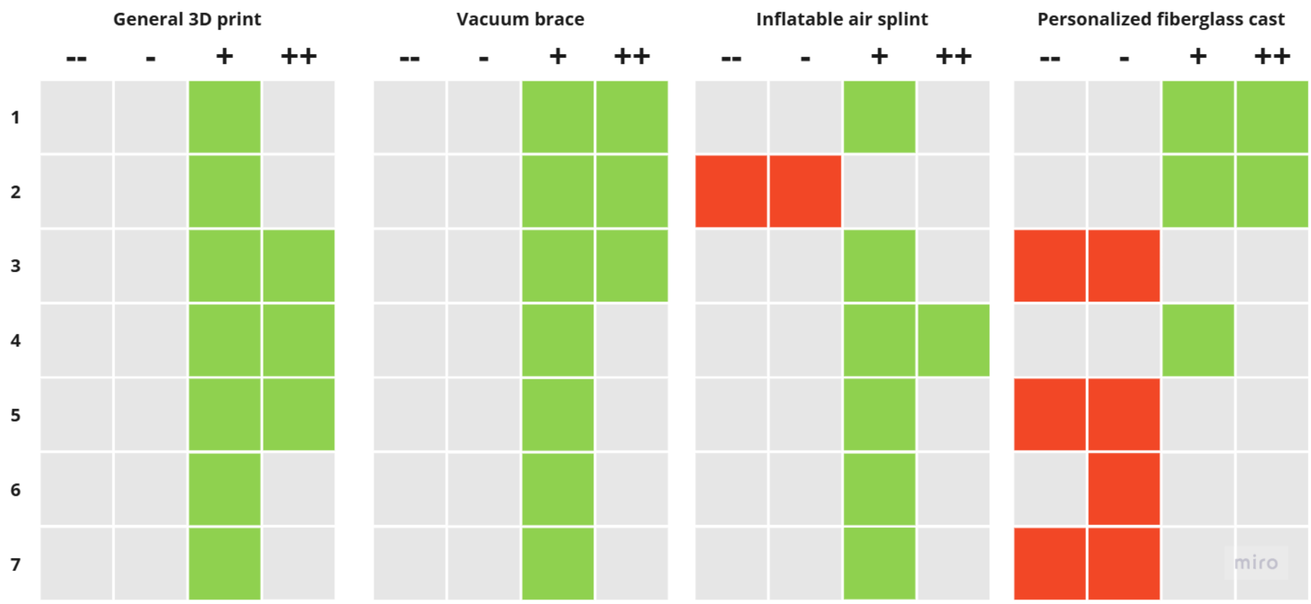

Fig. 12: Results of Harris profile evaluation

Appendix C: Prototypes

This appendix provides an overview of the prototyping phase, including visual documentation of key iterations leading to the final vacuum brace design. Photographs and annotated images illustrate the functional development, material choices, and modifications made in response to practical testing. These iterations were used to refine the fixation quality, usability, and robustness of the design before validation in the experimental setup.

Existing vacuum brace: PAX

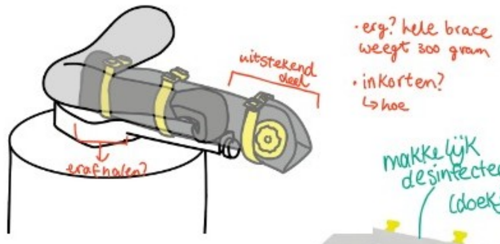

Prototype 1: Initial test of principle

- Vacuum bag filled with EPS beads.
- Wrapped around forearm and hand
- Vacuumed with vacuum cleaner
- Closed around arm with tape

Prototype 2: Velcro straps, smaller

- Less EPS beads: 2 cm thick
- Wrapped around forearm and hand : 32 cm
- Vacuumed with vacuum pump
- Closed around arm with three velcro straps

--> Beads can accumulate and form spots with less beads. Creating less stiff spots of the brace. How do you distribute the beads evenly?
--> Brace does not form to arm completely, forming with hand, when the brace is partially vacuum is needed
So therefore: straps need to be surrounding the arm. Especially at the top, bottom and wrist sections the brace needs to be formed to the shape of the arm.
--> still a bit to long (whole hand is in the brace) and probably to big for smal arms. For the circumference, it fits my arm, but probably is too small to close for bigger arms.
--> where do you put the clamp if you do not know where your wrist is in the brace? Some sort of indication for alignment is needed.

Prototype 3: Indication for alignment

- Several options
- Partial glove and rings are not easily cleanable
- Hand drawing is not suitable for left and right hands
- Chosen: simple line for wrist and clamp alignment

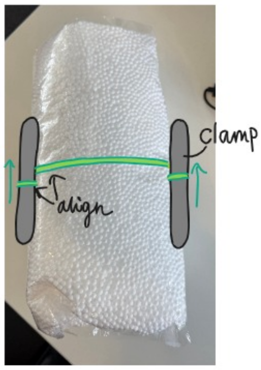

Prototype 4: EPS bead distribution

Will an inner fabric bag with compartments evenly distribute the EPS beads without decreasing the stiffness of the brace?

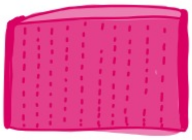

Version 1: non-elastic fabric, 6 vertical compartments: 28 x 33 cm

2 cm thick (while vacuumed)
about 200 ml EPS beads per compartment

Elastic fabric shows less dents at stitches: less weak spots along stitches.

Version 2: elastic fabric, 6 vertical compartments: 28 x 33 cm

2 cm thick (while vacuumed)
about 200 ml EPS beads per compartment

Try more compartments : thinner brace and better distribution of EPS beads

Try different measurements: based on anthropometric data and shrikage of brace when vacuuming, and place the valve in the corner of the brace

Version 3 and 4: elastic fabric, 8 vertical compartments: 25 x 35 cm

1.6 cm thick while vacuumed
150 ml per compartment
Felt too fragile

1.9 cm thick while vacuumed
160 ml EPS beads per compartments

Version 4 is the best option, but bending tests revealed that the brace was less stiff in the direction perpendicular to the stitches compared to the direction parallel to the stitches...

Prototype 5: Surrounding straps and outer cover

Outer cover should be waterproof, easy to clean and soft on the skin: oilcloth of HEMA. The vacuum bag with EPS beads is put inside the cover. The cover can be used to stitch straps on. This is not possible on the vacuum bag as is would cause leakage of air.

Surroundig elastic velcro straps form the brace to the shape of the arm, but elastic properties of the straps limit thightness possibilities. --> non elastic straps

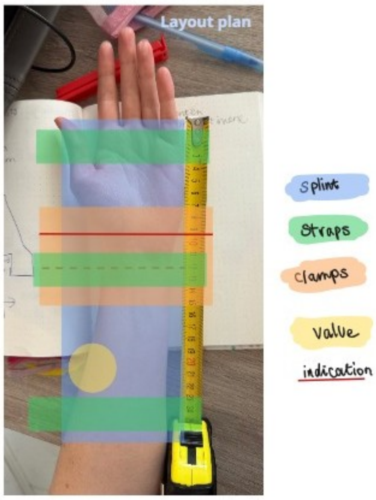

Prototype 6: Diagonal compartments and drawstrings

45 degrees diagonal compartments. Same outer dimensions, width of compartments and same total amount of beads as version 4 of prototype 4. Amount of beads per compartment was calculated for even distribution per cm^2

Bending tests showed roughly the same stiffnes in the x and y direction. Which wasn't the case for the version with vertical components.

Non-elastic drawstrings made it easy to form brace to the shape of arm thightly. But because the brace could still glide upen itself and inside the outer cover when forcing your arm to move inside the brace, the brace could bend in the x direction and slight supination, pronation and bending in the x direction if the arm was possible inside the brace.

--> therefore the brace needed two kinds of thightening straps. One that forms to the shape of the ar, (drawstrings) and one that encloses the U shape of the brace to an O shape to prevent gliding of the brace. This is specifically important at the top and bottom of the brace. Also the outer cover should be attached to the vacuum bag, prevening gliding of the vacuumbag inside the cover.

Prototype 7: Glued cover, straps and draw strings, indication line added

Final prototype

Laced draw strings

Prototype in clamps

Indication lines on inside and outside of brace

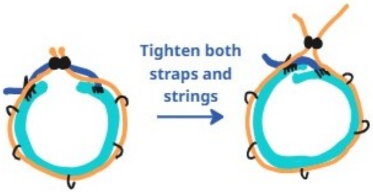

Outer cover plan

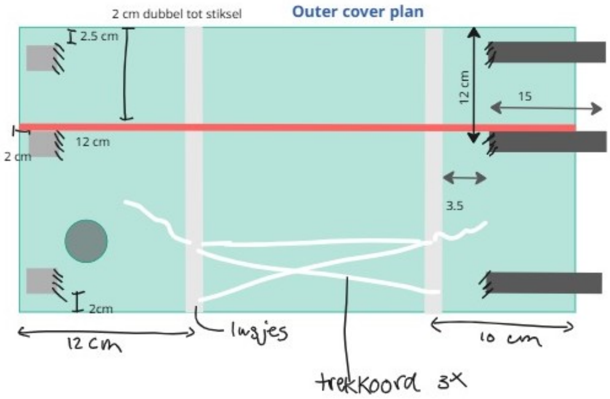

Appendix D: Vertical compartment

This appendix illustrates the internal layout of the vertical compartments within a vacuum brace prototype, as shown in Figure 13. These compartments were introduced to improve longitudinal stiffness and prevent deformation under axial loading.

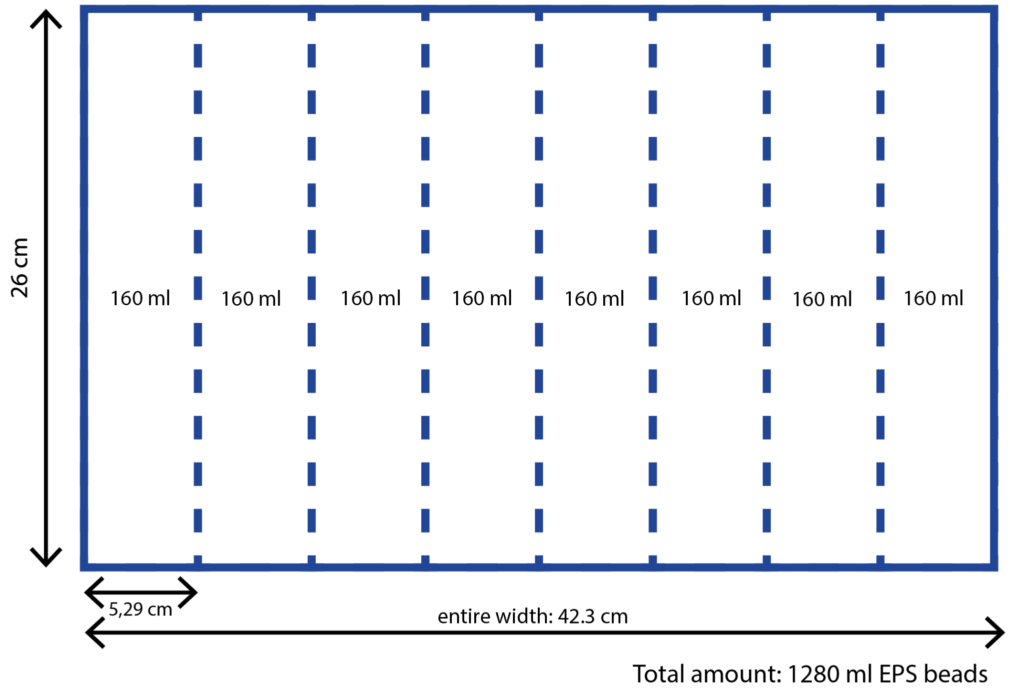

Fig. 13: Vertical compartments design

Appendix E: Bending tests

Bending tests were conducted to evaluate the stiffness of different flat vacuum brace concepts. Figure 14 illustrates the experimental setup. The brace was clamped in place with 10 cm extending beyond the fixture. A known weight (P) was applied to the end free segment. The resulting deflection was recorded and used to calculate the stiffness in terms of Young's modulus (E). Measurements were performed in both the longitudinal (L) and transverse (T) directions of the brace. The specific results and corresponding calculations, and derivation (Figure 15) are presented below.

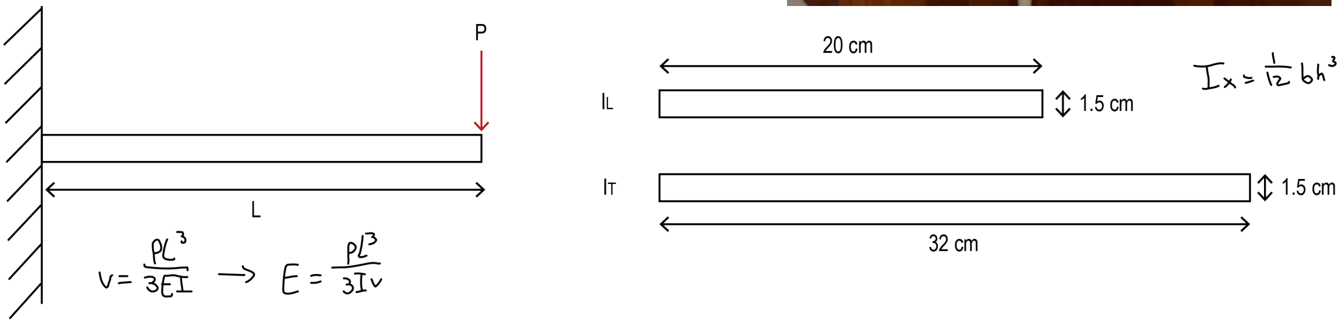

Fig. 15: Derivations of Young's modulus calculations

No compartments - 1300 ml EPS beads

$P_1 = 0.295kg * 9.81 = 2.89395N$

$L = 0.1m$

$I_L = \frac{1}{12}bh^3 = \frac{1}{12} * 0.2 * 0.015^3 = 0.000000056$

$I_T = \frac{1}{12}bh^3 = \frac{1}{12} * 0.32 * 0.015^3 = 0.00000009$

$v_L = 0.017m$

$v_T = 0.009m$

$E_L = \frac{2.9*0.1^3}{3*I_L*0.017} = 1015406.162Pa$

$E_T = \frac{2.9*0.1^3}{3*I_T*0.009} = 1193415.638Pa$

Vertical compartments - 1300 ml EPS beads

$P_2 = 0.396kg * 9.81 = 3.884765N$

$v_{Lv} = 0.017m$

$v_{Tv} = 0.035m$

$E_{Lv} = \frac{3.9*0.1^3}{3*I_L*0.017} = 1365546.218Pa$

$E_{Tv} = \frac{3.9*0.1^3}{3*I_T*0.035} = 412698.4127Pa$

Diagonal compartments - 1300 ml EPS beads

$P_2 = 0.396kg * 9.81 = 3.884765N$

$v_{Ld} = 0.018m$

$v_{Td} = 0.012m$

$E_{Ld} = \frac{3.9*0.1^3}{3*I_L*0.018} = 1289682.54Pa$

$E_{Td} = \frac{3.9*0.1^3}{3*I_T*0.012} = 1203703.704Pa$

Appendix F: Alignment options

Several alternatives were considered to achieve consistent wrist alignment within the brace. These options are explained below:

- Internal glove: An inner glove ensured that the hand and wrist always occupied the same position in the brace. However, this solution was impractical as it did not accommodate both left and right hands and complicated cleaning procedures.
- Alignment ring**s**: Soft silicone rings placed at the thumb and little-finger positions inside the brace guided wrist placement. Although this method was compatible with either hand, the rings would complicate routine cleaning with simple surface disinfection.
- Hand-outline imprint: A printed silhouette of a hand on the inner surface provided a quick visual guide for hand placement. This method was unsuitable due to limited adaptability to different hand sizes and the need for separate patterns for left and right hands.
- Reference line: A single line, drawn in contrasting color on both the inner and outer surfaces at the level of the wrist indents, marked the correct wrist position. The external line also serves as a guide to align the brace with the SEP.

Based on these considerations, the reference line was adopted due to its simplicity, compatibility with both hands, and minimal impact on cleaning procedures.

Appendix G: 3D model of clamp

Based on the original clamp design mounted to the SEP arm, the clamp was modified to accommodate an arm fitted with the vacuum brace. In addition, the clamp was widened to increase the fixation surface area. The final design is shown in Figure 16.

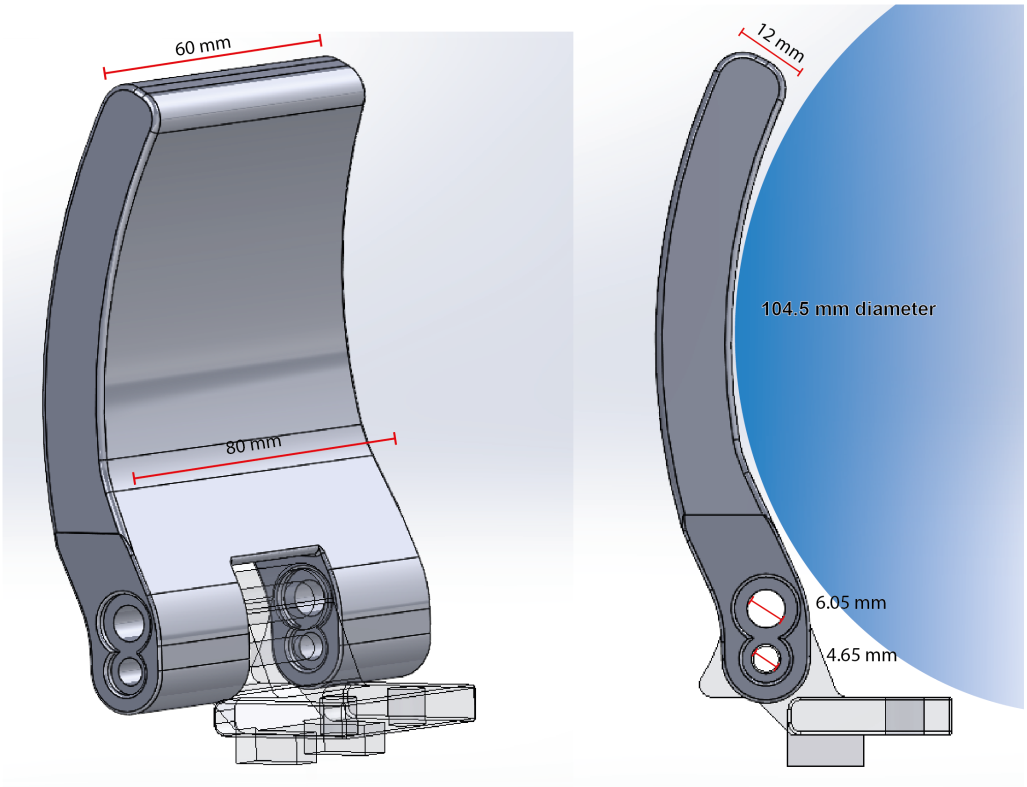

Fig. 16: redesigned clamps for fixating the vacuum brace into the SEP

Appendix H: Instructions vacuum brace usage

Instructions for using the vacuum brace are shown in Figure 17 below.

Ensure the brace is slightly unfolded, with the red indication line on the interior visible.

Guide the patient's arm into the brace, aligning the wrist indentations with the red indication line on the brace.

Secure the straps into the clips and tighten them a bit. Tighten the draw strings as well, forming the brace to the shape of the arm.

Unscrew the valve cap and attach the vacuum pump.

Pump approximately three times to partially stiffen the brace, making the brace slink a bit.

To account for the slinking: re-tighten the straps and strings securely, ensuring the brace conforms closely to the patient's arm.

Use the vacuum pump to remove the remaining air, pumping approximately seven times until the brace becomes completely rigid. Detach the vacuum pump

Tuck any excess strings into the designated pocket for a tidy setup.

Align subject in the SEP as specified. Adjust the position of the clamp so the red line on the brace aligns with the red line on the clamp, then tighten the clamp securely, ensuring it is firm but does not cause discomfort to the patient. Execute your measurements

Fig. 17: Step by step instructions for applying the vacuum brace prototype to a subject.

To release the subject: loosen the clamps to release the patient from the SEP. Then, loosen the straps and draw strings, and release the vacuum by using your finger to alter the shape of the valve, allowing air to flow back into the brace.

Appendix I: Creating the final prototype

The final vacuum brace prototype was manufactured using the following step-by-step process:

1) The final prototype of the vacuum brace was constructed using a vacuum bag obtained from 'De Vacuumzakken Specialist'. The bag was heat-sealed to a final size of 25 cm by 36 cm, with the valve positioned in one corner to avoid interference with clamps or straps during application. These dimensions ensure compatibility with both small and large forearms and wrists. The vacuum bag contains a compartmentalized inner sleeve filled with EPS beads.
2) The compartmentalization was achieved by sewing diagonal channels into an elastic fabric cover using a sewing machine. The compartments were oriented at a 45-degree angle and spaced 5.3 cm apart. The top and one side of the fabric were left open to allow the insertion of EPS beads using a funnel. A total volume of approximately 1300 mL of EPS beads was distributed evenly across nine compartments to ensure uniform stiffening. These compartments prevent lateral migration of beads and contribute to consistent mechanical behavior across the brace.
   Figure 18 illustrates the diagonal compartment structure used to stabilize the EPS bead distribution. Figure 19 shows the inner vacuum bag with the outer cover and all relevant design features.

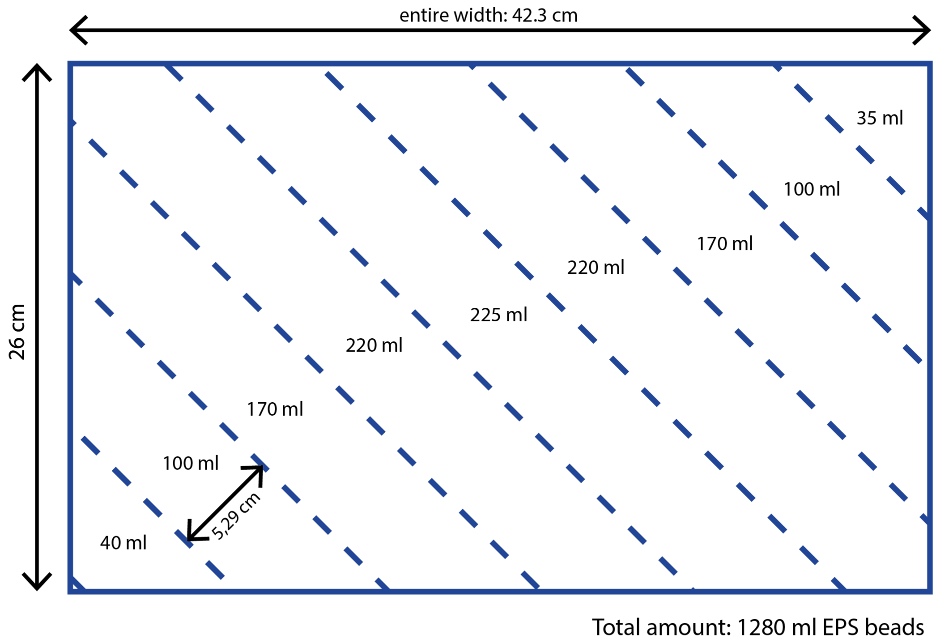

Fig. 18: Inner elastic fabric sleeve with nine diagonal compartments filled with EPS beads. The 45-degree orientation enhances rigidity by resisting transverse bending.

3) A piece of waterproof tablecloth fabric (HEMA) was sewn onto the top of the vacuum bag to form the outer support cover. A curtain tape (HEMA) was stitched onto the surface to serve as lacing guides. Additionally, three adjustable tension straps with buckles were attached at the top, middle, and bottom for secure fixation. A small elastic loop was included to manage excess lace material.
4) Three nylon laces, each 150 cm in length, were threaded in a crisscross pattern through the sewn loops, enabling even tightening around the arm. The laces were secured with double cord stoppers for ease of use. A red line was drawn on both the interior and exterior surfaces of the brace using a waterproof marker to indicate the correct wrist alignment position.
5) Due to the vacuum forming process and the volume taken up by the EPS beads, the brace dimensions were determined iteratively through trial and error. After vacuum compression, the final external dimensions of the brace matched the intended 24 cm by 35 cm size.

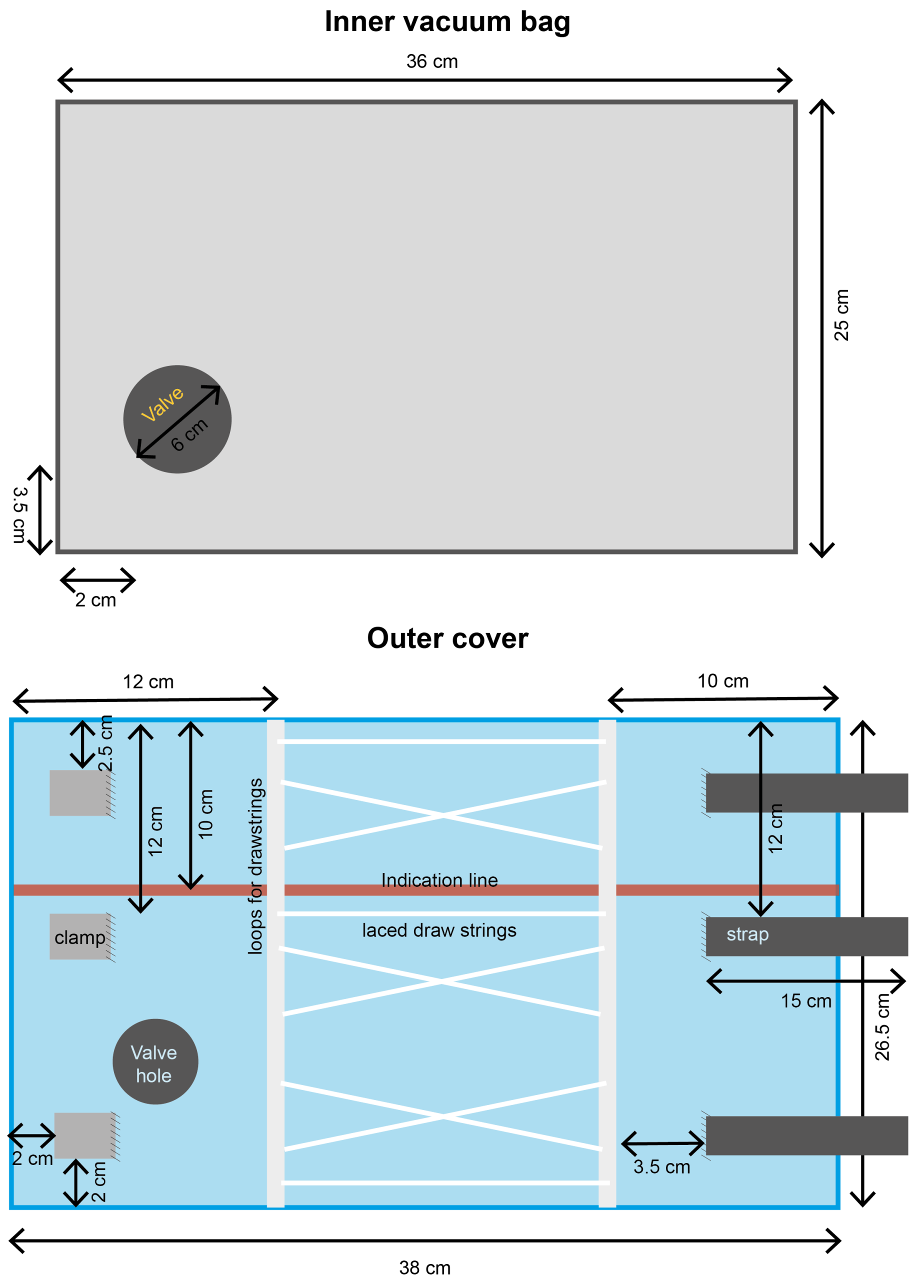

Fig. 19: Final construction of the vacuum brace showing the inner vacuum bag with the compartmentalized bead sleeve and the attached outer layer with fixation features.

Appendix J: Participant information

Participant information - System performance analysis of the Shoulder Elbow Perturbator using a vacuum brace

You are invited to participate in the study 'Performance and comfort analysis of the shoulder elbow perturbator using a vacuum brace'. This is a study conducted by Jet Meijers.

Study objective

The objective of this study is to assess the shoulder elbow perturbator's (SEP) performance and comfort in identifying human elbow joint properties using a vacuum brace, shown in Figure 1 at the bottom of this document. The study will involve perturbations of the elbow and free movement of the elbow in interaction with the device.

What is expected of you?

During the session of approximately 1h of work, you will undergo perturbations and active movement of the elbow joint during different experimental conditions in the SEP. The SEP is shown in Figure 2 at the bottom of this document. The following experimental conditions will be performed:

- Passive multisine rotational perturbation of the elbow joint, with a 5 degree amplitude, and a 0.1 - 100Hz bandwidth. These multisine perturbations also feel as a random low amplitude vibration of the arm. However during these perturbations you are asked to **relax the elbow**. (1 repetitions of ~220 seconds)
- Multisine torque perturbation of the elbow joint, with the torque amplitude normalized to keep elbow joint rotation <5deg, and a 0.1-100Hz bandwidth. These perturbations will feel like random low amplitude vibrations. During this experiment you are asked to **resist the perturbations**. (2 repetitions of ~120 seconds, 30 seconds rest between the repetitions)
- Passive flexion and extension stretches of the elbow joint through its full passive range of motion, at velocities a velocity of 6 deg/s. You are asked to **match your force** , displayed with a blue line on the monitor to the yellow target line on the monitor. (9 repetitions of ~40 seconds, 10 seconds rest between the repetitions)
- Passive flexion and extension stretches of the elbow joint through its full passive range of motion, at velocities a velocity of 200 deg/s. You are asked **to match your force** , displayed with a blue line on the monitor to the yellow target line on the monitor. (9 repetitions of ~40 seconds, 10 seconds rest between the repetitions)

While you are seated next to the device, your arm (with or without brace) will be strapped in and perturbed by the SEP. After the experiment you will be asked to fill in a short questionnaire about your comfort during the tests. The experiment conditions will be repeated twice. Once with the your arm fixated in a vacuum brace and once without.

During the experiment 3 OptiTrack cameras are pointed at your arm from different angles. The cameras will detect the 7 reflective markers that will be stuck on your shoulder, elbow, forearm and fingers.

Before starting the experiments, you are asked to generate as much force as possible on the device while the handle is kept still three times. Furthermore, your passive range of motion is determined by flexing and extending the elbow joint within a comfortable range. These measurements are used to set the device's safety limits, and benchmark your measured data.

What data will be acquired?

During all experiments, the rotation of the device (and your attached elbow) and the force you exert on the device will be collected. The force can be used to determine your elbow joint torque. Together, rotation and torque of the elbow can give us information on the stiffness, damping, and inertial properties of your elbow. The three motion tracking cameras will only record the location of the markers on your skin during the experiments. There will be no video footage of you acquired. These locations will be used to analyze the movement of your arm during the experiments.

At the beginning of the experiment your wrist circumference, forearm circumference, and forearm length will be measured and noted. Additionally, at the end of the experiments, questions about your comfort during the session will be asked and noted.

What happens to the data?

Your data will be pseudonymized with a unique number, thereby dissociating the data from directly identifiable information such as your name. After one week, the unique number linking your torque or rotation data to your name will be deleted. This means that upon request, you can only have your data deleted in the first week after the experiment, as after this period, it will be untraceable. The data will be used for research that may be published in an international scientific journal.

To reduce the possibility that your age and gender lead to your re-identification, your exact age will not be stored. Instead, you will be assigned to an 'age group' (e.g. 18-25, 25-35 etc.). Your age group and gender will be stored together with the torque- and rotation data for further research.

What are the risks associated with this study?

This device perturbs your elbow-joint by moving the under-arm. In case of a device malfunction, the possibility of overstretching the elbow joint may arise. However, the device has multiple safety mechanisms built in to prevent this overstretching from happening:

- Mechanical end-stops within the device, not allowing the device to rotate the elbow joint further than the mechanical end-stop location. These will be set at the limits of your passive range of motion.
- Virtual end-stops within the software, shutting down the motors at 5 degrees before the mechanical end-stop.
- A safety button in reach of both you and the researcher at all times during the experiment. Pressing this safety button shuts down the motors immediately

The use of the vacuum brace involves certain potential risks. The possibility of the brace being applied too tightly, which could lead to temporary discomfort for the participant. Moreover, in the event of an emergency requiring the rapid release of the participant's arm, the brace may continue to restrict movement of the arm, wrist, and hand, thereby limiting immediate mobility. To mitigate these risks the following safety policies are present:

- You will be asked to provide real-time feedback during the application process to ensure that the brace is not overly constrictive.
- In emergency situations, the brace itself can be swiftly detached from the SEP, allowing the participant to exit the setup. Furthermore, the brace can be released via a valve, enabling rapid removal of the brace and restoration of full limb mobility. This can be seen in Figure 3.

If you are experiencing elbow pain or currently have an elbow injury, the perturbations could lead to serious discomfort or even pain. Therefore, in the case of an elbow injury you are not allowed to participate in this study.

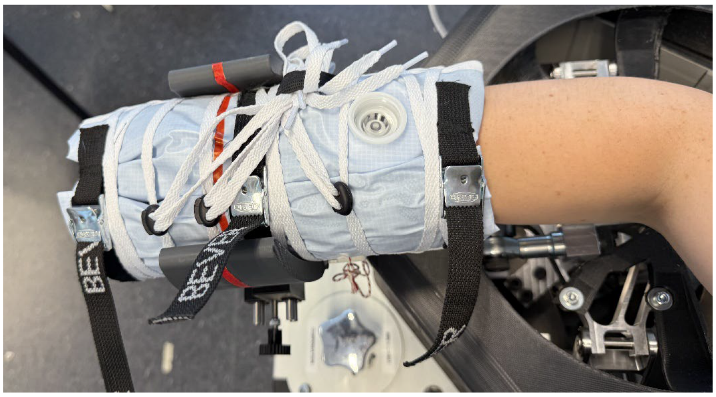

Figure 1: Vacuum brace

Figure 2: The Shoulder Elbow Perturbator

Figure 3: Valve of vacuum brace

Appendix K: Informed consent

TU Delft – Faculty Mechanical Engineering (ME) Mekelweg 2, 2628 CD Delft Tel: +31 (0)15 27 89809

Consent Form SEP-perturbation experiment

For participation in the study: 'Performance and comfort analysis of the shoulder elbow perturbator using a vacuum brace'

Please check the appropriate box

Participation in the study	**Yes**	**No**
I have read and understood the participant information from 05/2025. I have asked my questions about the study, and they have been answered to my satisfaction.		
I voluntarily consent to participate in this study as a participant, and I understand that I can refuse to answer questions and that I can withdraw from the study at any time without giving a reason.		
I understand that participation in the study involves undergoing mechanic elbow perturbations.		
I understand that there is no compensation for my participation.		
I understand that taking part in the study involves the following risks, as described in the participant information, namely: - Overstretching of the arm, causing pain or injury - The vacuum splint might be applied too tightly, causing temporary discomfort - In case of an emergency my arm, wrist, and hand may still remain immobilized in the splint, reducing immediate mobility of the hand and wrist - The adhesive of the reflective markers may cause skin irritation - Feeling uncomfortable having three motion-tracking cameras pointed at me I understand that these will be mitigated by numerous safety policies present as described in the participant information, namely: - Virtual end-stops for the device based on sensor information - Mechanical end-stops for the device prohibiting further elbow rotation - An emergency button within reach of both participant and researcher - I will be asked to provide immediate feedback during the application of the splint to ensure it is not overly tight - In an emergency, the splint can be quickly detached from the SEP, allowing me to move away from the setup. Additionally, the vacuum splint can be quickly released using the valve - I am informed in advance about the placement of the markers and asked about allergies or sensitive skin. - The OptiTrack cameras only record the location of the reflective markers and do not capture visual images of the participant during the experiment.		
(Further) use of information/data in the study		
I understand that taking part in the study also involves collecting specific personally identifiable information (PII), specifically my name, sex, and age, with the potential risk of my identity being revealed.		
I understand that the following steps will be taken to minimize the threat of a data breach, and protect my identity in the event of such a breach: - Anonymization of data through using a 'key' linked to my data, instead of my name. The link between 'key' and name is removed one week after data collection. - Storing all information, and the link between the 'key' and my name, on a secured project drive, instead of locally on a laptop.		
I understand that, for confidentiality reasons, all information that could lead to linking my identity to my measurement data will be removed. Therefore, I have a one-week period to request the deletion of my data. After that, my data cannot be retraced.		
I understand that the data I provide will be used for a possible publication in an international scientific journal.		

1/2

I understand that the personal information that can identify me, like my name and age, will not be shared outside the study team.		
I give permission to the research team to archive all data (age, gender, kinetic measurements) that has been collected from me, to use for future research and learning.		

Name of participant Signature Date

I, as researcher, have accurately read out the information to the potential participant. I did my utmost to ensure that the participant understands what they are voluntarily consenting.

Name of researcher Signature Date

Appendix L: Comfort questionnaire

Comfort questionnaire SEP measurements

Participant nr: ________

Wrist circumference:____________
Forearm circumference:____________
Forearm length:____________

Age: ☐ 18- 25 ☐ 26 - 35 ☐ 36 - 45 ☐ 46 - 60 ☐ 60+

Gender: ☐ Female ☐ Male ☐ Other

1. How would you rate the overall comfort during the tests?

Without brace:	☐	☐	☐	☐	☐
With brace:	☐	☐	☐	☐	☐
	1 No discomfort	2 Slight discomfort	3 Moderate discomfort	4 Severe discomfort	5 Unbearable discomfort

2. How would you rate the comfort of specific body parts during/after the tests?

Without brace:

Elbow	☐	☐	☐	☐	☐
Forearm	☐	☐	☐	☐	☐
Wrist	☐	☐	☐	☐	☐
Hand	☐	☐	☐	☐	☐
	1 No discomfort	2 Slight discomfort	3 Moderate discomfort	4 Severe discomfort	5 Unbearable discomfort

With brace:

Elbow	☐	☐	☐	☐	☐
Forearm	☐	☐	☐	☐	☐
Wrist	☐	☐	☐	☐	☐
Hand	☐	☐	☐	☐	☐
	1 No discomfort	2 Slight discomfort	3 Moderate discomfort	4 Severe discomfort	5 Unbearable discomfort

3. Did you experience any sensations of pinching, pressure points, or other discomfort? If so, where exactly?

Without brace:

____

With brace:

4. Was there a specific moment when it became more uncomfortable? For example, during a particular measurement or task? (Feel free to ask for help if you're unsure how to describe the measurement/task.)

Without brace:

With brace:

5. What measurements did you prefer, with or without the brace?
   Without brace / With brace

Appendix M: Forearm rotation analysis

To compute supination and pronation, OptiTrack marker trajectories from the forearm and the left and right SEP clamps were used. The anatomical rotation axis of the forearm was determined at each time step to track torsion over time. The procedure was as follows:

- The unit x-axis of rotation was defined as the normalized vector from the midpoint between the two clamp markers to the forearm marker.
- A temporary y-direction was computed as the normalized vector between the left and right clamp markers.
- The cross product of the x- and temporary y-vectors yielded a provisional z-axis, which was normalized.
- The corrected y-axis was computed as the cross product of the z- and x-axes.

These three orthonormal vectors formed the instantaneous rotation matrix R at each time step. The first valid rotation matrix served as a reference matrix R_{ref}. For each subsequent time point, the relative rotation matrix R_{rel} was computed as:

$$R_{\text{rel}} = R_{\text{ref}} \cdot R$$

The torsion angle around the anatomical x-axis was extracted from R_{rel}, resulting in a time series of absolute forearm rotation angles. Figure 20 shows a screenshot of the motion capture data in Motive, illustrating the definition of the anatomical rotation axis and the associated coordinate system.

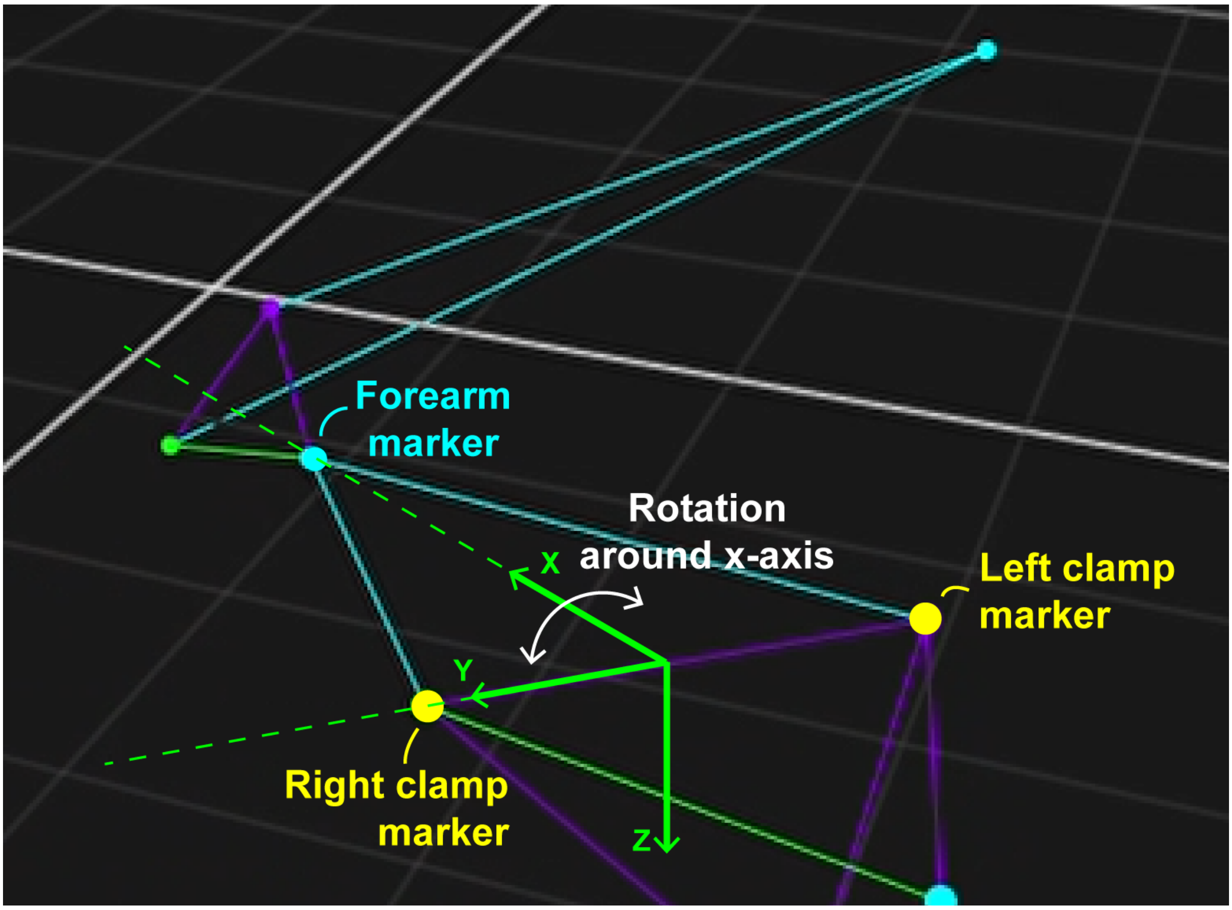

Fig. 20: Definition of the rotation axis.

Appendix N: Comfort questionnaire results

This appendix shows the answers of every participant to the questions from the comfort questionnaire in tables.

TABLE III: Q1 – How would you rate the overall comfort during the tests?

Participant	Without Brace	With Brace
1	3	2
2	3	2
3	4	2
4	4	2
5	3	2
6	4	2
7	4	1
8	4	2
Mean	3.625	1.875
SD	0.518	0.354

TABLE IV: Q2 – How would you rate the comfort of specific body parts during/after the tests?

Participant	Elbow		Forearm		Wrist		Hand	
	Without brace	With brace	Without brace	With brace	Without brace	With brace	Without brace	With brace
1	4	2	1	2	3	2	1	2
2	1	1	1	2	4	2	2	2
3	1	2	1	1	4	1	3	1
4	1	1	1	1	5	2	1	1
5	1	1	1	1	3	1	1	1
6	1	3	1	1	4	1	1	3
7	2	3	2	1	5	1	1	1
8	1	1	1	1	4	2	1	2
Mean	1.5	1.75	1.125	1.25	4.0	1.5	1.375	1.625
SD	1.07	0.89	0.35	0.46	0.76	0.53	0.74	0.74

TABLE V: Q3 – Did you experience any sensations of pinching, pressure points, or other discomfort? If so, where exactly?

Participant	Without Brace	With Brace
1	Pressure point at my wrist, and my skin got stuck there	On my elbow there was a pressure point and there was some pressure on my arm but I got used to that quickly
2	Mainly discomfort around my wrist (where the clamps were) towards my hand, a lot of pressure there	With brace it really fit better around my wrist. Of course, it sits tight, but it didn't really hurt anywhere.
3	Ja, pols binnenkant onder de duim zit een drukpunt van de klem.	Yes, inside of the wrist under the thumb there was a pressure point from the clamp.
4	I felt an enormous sensation of discomfort and even pain in my wrist when exerting force on the clamp	No, discomfort was severely decreased. No pressure points whatsoever.
5	I did have some pressure points on the area between wrist and most broad part of the hand.	It was very warm but did not hurt
6	At wrist especially on the outside	Pressure point on elbow, pinching of hand
7	Pain at the side of the wrist on the thumb side (even a small cut)	At the elbow some pressure on the support point at the start
8	Side of my wrist, below my thumb hurt because of the clamp and extra when applying force	A bit at my wrist below my thumb it felt a bit uncomfortable

TABLE VI: Q4 – Was there a specific moment when it became more uncomfortable? For example, during a particular measurement or task?

Participant	Without Brace	With Brace
1	During stretch (50%) I felt a shock through my elbow	No, I do not know a specific moment
2	Mainly annoying at the end; more discomfort after applying force for longer	Felt my elbow at the end, possibly from sitting long
3	With high speeds of stretch tests; worse with 50% force	It was heavier but not more painful when faster
4	Discomfort during max force and 50% force stretches	Brace distributed pressure so discomfort vanished
5	Nope	Maybe little bit due to temperature
6	Yes, at 25% and 50% stretch tests at the inside of the wrist	Pinching of hand increased toward end of tests
7	Pain during stretch tests with force. Could not finish	Not uncomfortable but had to follow yellow line
8	Hurt most during 50% force stretch test	At moments with high force

TABLE VII: Q5 – What measurements did you prefer, with or without the brace?

Participant	Comment
1	with brace
2	with brace
3	with brace
4	with brace
5	with brace
6	with brace
7	with brace
8	with brace

Appendix O: Extra result data

This appendix shows additional results from the data acquired from the experiments. Table VIII shows the maximal voluntary torque measurements during the measurements.

TABLE VIII: Comparison of MVT with and without brace

Participant	Without - 1	Without - 2	Without - 3	Without - Mean	With - 1	With - 2	With - 3	With - mean
1	43	39	32	38.00	31	34	35	33.33
2	28	36	26	30.00	29	27	28	28
3	25	22	18	21.67	34	33	29	32
4	31	33	29	31.00	47	39	37	41
5	13	11	8	10.67	9	10	11	10
6	16	18	17	17.00	20	20	18	19.33
7	17	19	20	18.67	16	16	20	17.33
8	21	23	25	23.00	33	35	27	31.67
Mean	24.25	25.13	21.88	23.75	27.38	26.75	25.63	26.58

Figure 21 shows the mean displacement of the lateral epicondyle marker with respect to the SEP pivot marker in the z-plane for all participants.

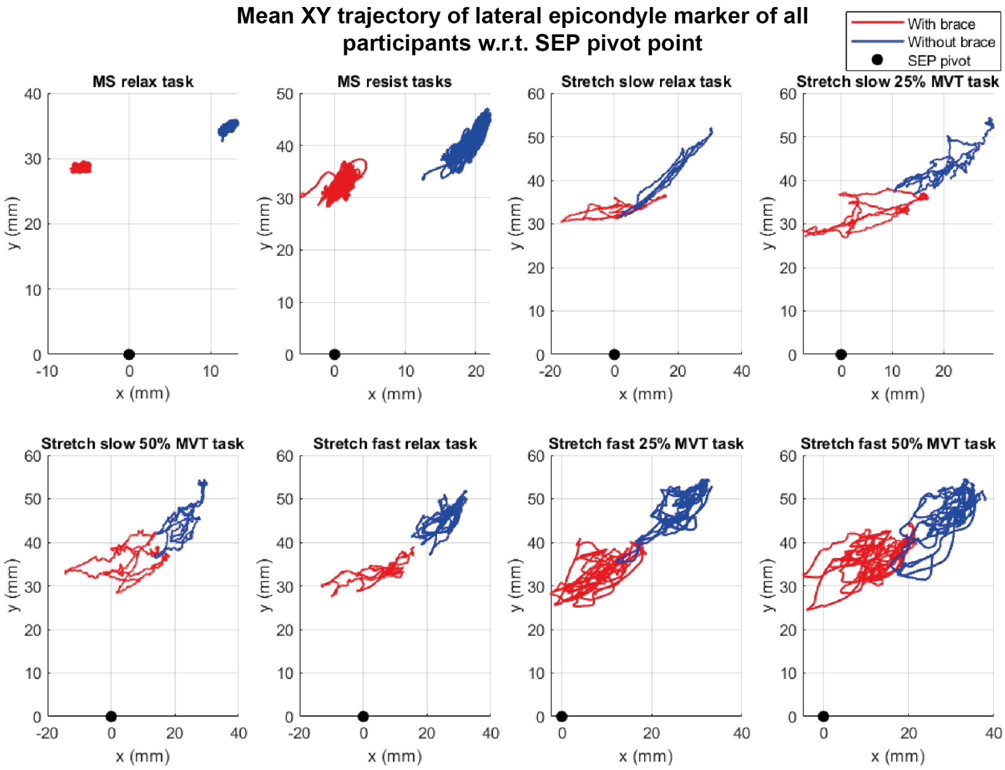

Fig. 21: Mean epicondyle displacement in z-plane

Figure 22 shows the mean RMS of the lateral epicondyle marker velocity with respect to the right clamp marker in the z-plane for all participants per task.

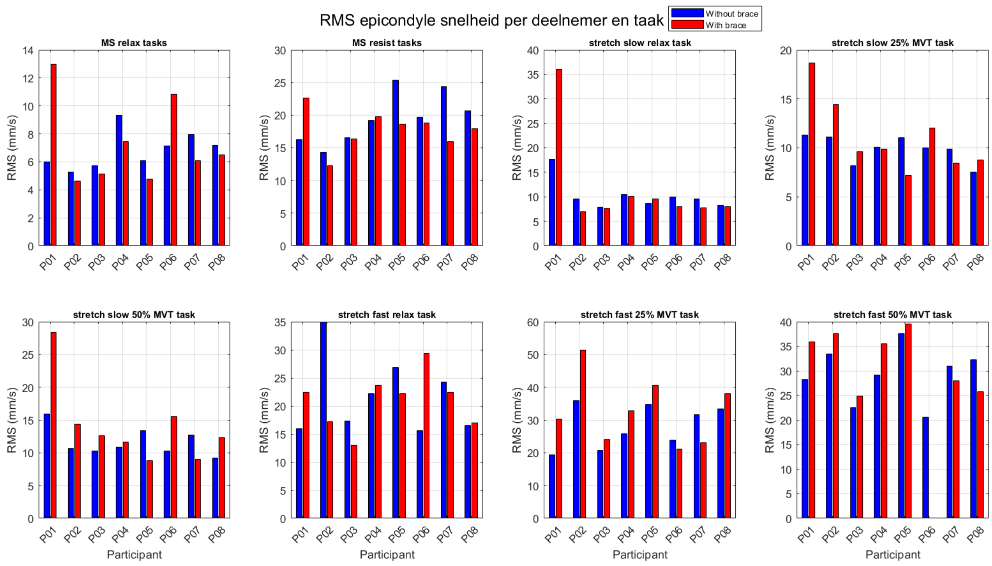

Fig. 22: RMS epicondyle velocity per task

Figure 23 shows the mean displacement of the finger markers with respect to the right clamp marker in the z-plane for an exemplary participant.

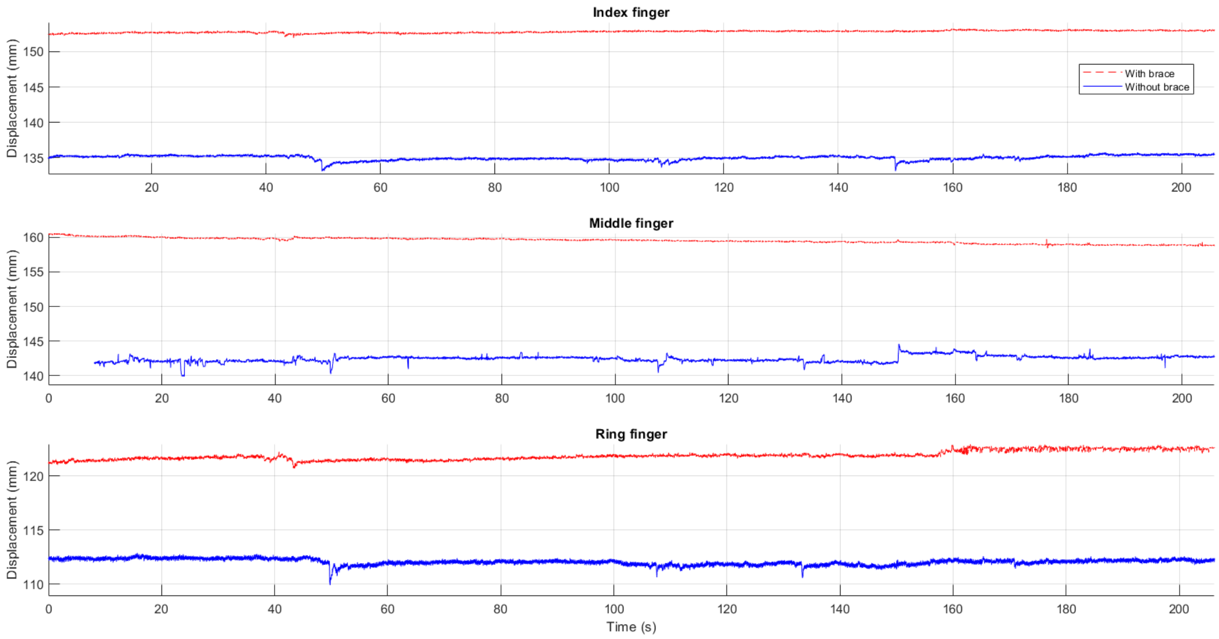

Fig. 23: Finger displacement in z-plane of an exemplary participant